CPL-Tunable BN-Embedded Supramolecular Macrocycles

Yu-Chi Dai, Yun-Tao Ding, Jin-Lin Qing, Wei-Ning Zhang, Zhi-Qiang Zhang, Xuefeng Zhu, Jing-Jing Cao*, Chun-Lin Sun, Xiao-Ping Cao* and Hao-Li Zhang*

State Key Laboratory of Applied Organic Chemistry (SKLAOC); Key Laboratory of Special Function Materials and Structure Design (MOE); College of Chemistry and Chemical Engineering, Lanzhou University, Lanzhou, 730000, P. R. China.

Corresponding Authors

Jing-Jing Cao E-mail: caojj@lzu.edu.cn.
Xiao-Ping Cao E-mail: caoxp@lzu.edu.cn.
Hao-Li Zhang E-mail: haoli.zhang@lzu.edu.cn.

1. General methods, instrumentation and techniques

All reagents were used without purification. Starting chemical substrates and reagents were used as commercially provided unless otherwise indicated. Thin-layer chromatography (TLC) was performed on silica gel and the chromatograms were visualized using UV light (λ = 254 or 365 nm). Flash column chromatography was performed using silica gel (200–300 mesh). ^{1}H and ^{13}C NMR spectra were recorded in CD_2Cl_2 solution, $CDCl_3$ solution or DMSO solution at 25 ºC, unless otherwise indicated. Chemical shifts are expressed in parts per million (δ scale). ^{1}H and ^{13}C NMR spectra are referenced to residual protons of CD_2Cl_2 as internal standard (δ = 5.32 and 53.84 ppm, respectively), $CDCl_3$ as internal standard (δ = 7.26 and 77.16 ppm, respectively) and DMSO as internal standard (δ = 2.54 and 39.5 ppm, respectively). The NMR was performed using Bruker Avance III 400 and Bruker Neo 600. The UV was performed using Hitachi U-3900. The FL was performed using Hitachi F-7000. High-resolution mass spectrometry (HRMS) was performed using electrospray ionization (ESI) and hybrid quadrupole time-of-flight mass detector (QTOF; positive-ion mode) for the detection, unless otherwise indicated. The circular dichroism (CD) was performed using JASCO J-1500 CD Spectrameter. The circularly polarized luminescence (CPL) was performed using JASCO CPL-300.

CD, CPL and total luminescence spectra were recorded at 20 ºC, unless otherwise indicated, on an instrument described previously, operating in a differential photon-counting mode.

2. Synthetics procedures and characterization data

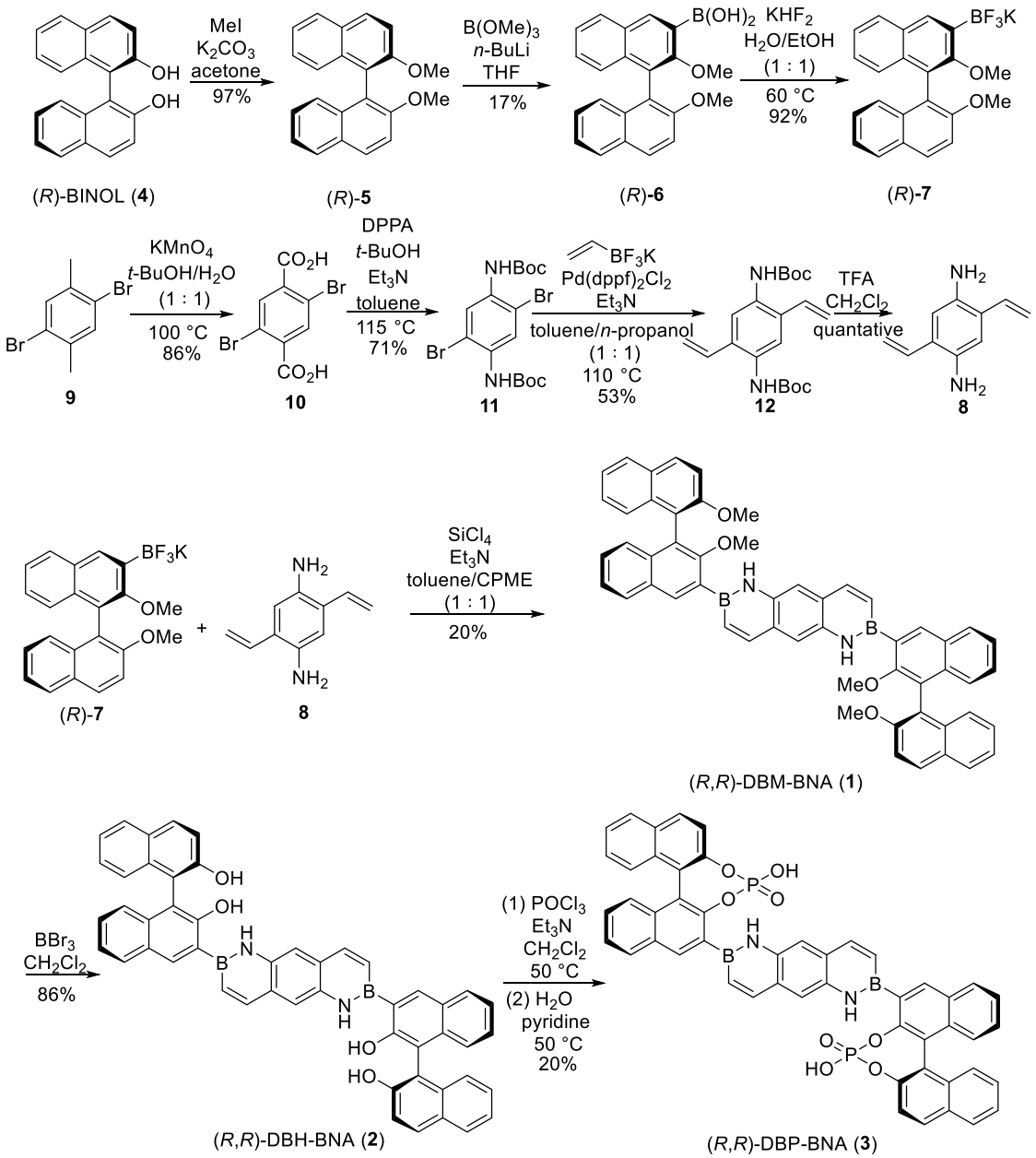

Scheme S1. Synthetic access to (*R,R*)-DBM-BNA (**1**), (*R,R*)-DBH-BNA (**2**) and (*R,R*)-DBP-BNA (**3**).

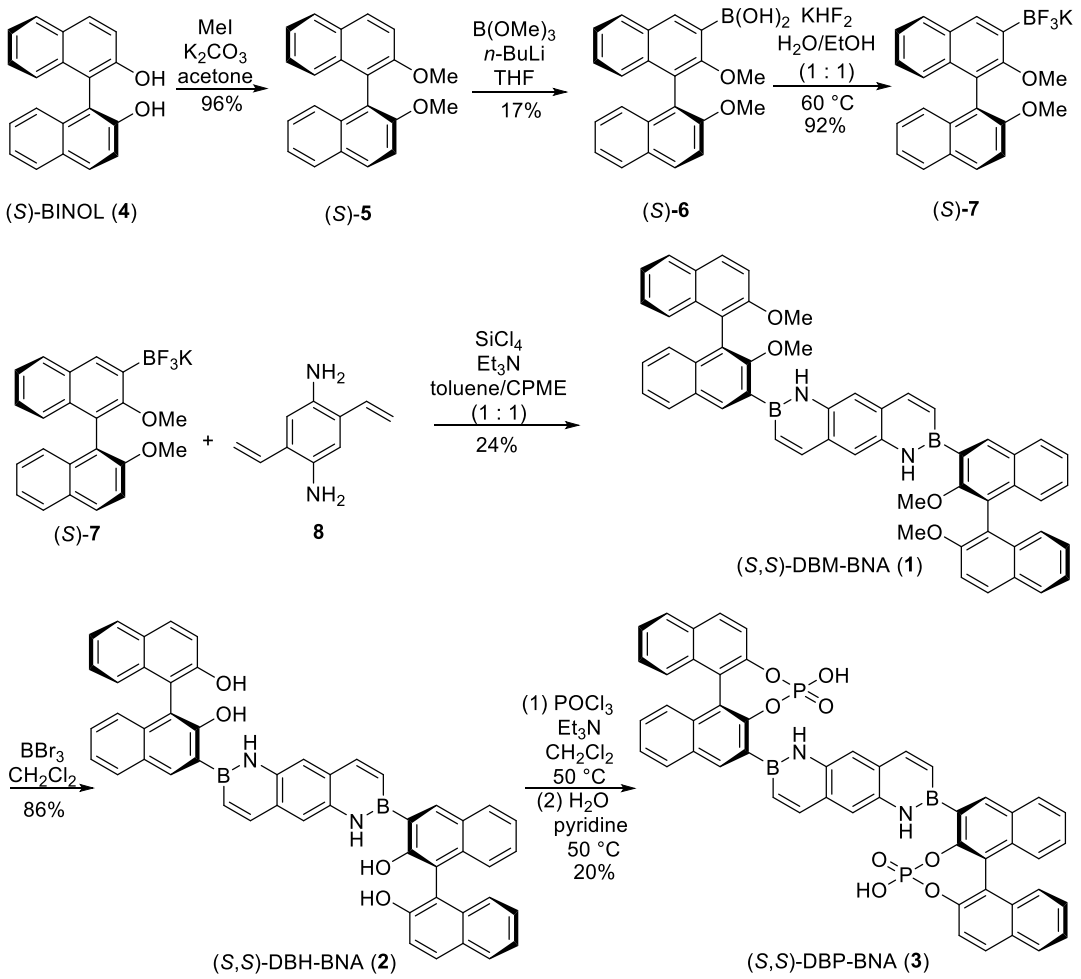

Scheme S2. Synthetic access to (*S,S*)-DBM-BNA (**1**), (*S,S*)-DBH-BNA (**2**) and (*S,S*)-DBP-BNA (**3**).

(*R*)-2,2'-Dimethoxy-1,1'-binaphthalene [(*R*)-5]

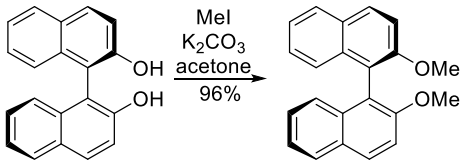

To a solution of (*R*)-[1,1'-binaphthalene]-2,2'-diol (**4**, 10.0 g, 34.96 mmol) in acetone (200 mL), potassium carbonate (16.5 g, 119.57 mmol) and methyl iodide (14.8 g, 104.22 mmol) were added. The reaction mixture was stirred at 70 °C for 36 h. Water (100 mL) was added and the formed precipitate was collected.[1] (*R*)-**5** was obtained as a white powder (10.6 g, 96%). m.p. = 197–198 °C. ^{1}H NMR (600 MHz, $CDCl_3$): δ = 7.98 (d, 2H, *J* = 12.0 Hz), 7.87 (d, 2H, *J* = 12.0 Hz), 7.46 (d, 2H, *J* = 12.0 Hz), 7.31 (t, 2H, *J* = 12.0 Hz), 7.21 (t, 2H, *J* = 12.0 Hz), 7.10 (d, 2H, *J* = 12.0 Hz), 3.77 (s, 6H). LRMS (ESI-TOF) *m/z* calcd for $C_{22}H_{18}O_2Na^+$ $[M + Na]^+$: 337.12, Found: 337.12.

(*S*)-2,2'-Dimethoxy-1,1'-binaphthalene [(*S*)-5]: according to the synthesis path and the method described of (*R*)-**5** above, (*S*)-**5** (10.5 g, 96%) was obtained from (*S*)-**4** (10.0 g, 34.97 mmol) as a white powder. m.p. = 197–198 °C. ^{1}H NMR (600 MHz, $CDCl_3$): δ = 7.98 (d, 2H, *J* = 12.0 Hz), 7.87 (d, 2H, *J* = 12.0 Hz), 7.46 (d, 2H, *J* = 12.0 Hz), 7.31 (t, 2H, *J* = 6.0 Hz), 7.21 (t, 2H, *J* = 12.0 Hz), 7.10 (d, 2H, *J* = 12.0 Hz), 3.77 (s, 6H). LRMS (ESI-TOF) *m/z* calcd for $C_{22}H_{19}O_2^+$ $[M + H]^+$: 315.14, Found: 315.14.

(*R*)-(2,2'-Dimethoxy-[1,1'-binaphthalen]-3-yl)boronic acid [(*R*)-6]

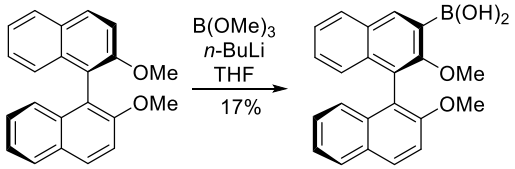

(*R*)-**5** (*R*)-**6**

To a mixture of (*R*)-**5** (5.00 g, 15.92 mmol) and tetrahydrofuran (100 mL), *n*-BuLi (7 mL, 2.5 M in hexane, 17.50 mmol) was added dropwise at room temperature. The mixture was stirred at room temperature for 12 h. Trimethyl borate (2.00 g, 19.20 mmol) was added. The reaction mixture was allowed to reach room temperature overnight. Hydrochloric acid (1 M, 100 mL) was added and stirred for 3 h at room temperature. The organic phase was separated and washed with hydrochloric acid (1 M, 40 mL × 2) and brine (50 mL). The organic phase was dried over $MgSO_4$, filtered, and all volatiles were removed under reduced pressure.[2] Flash chromatography of the residual through silica gel (dichloromethane, R_f = 0.1) afforded compound **6** (0.97 g, 17%) as a pale yellow powder. ^{1}H NMR (400 MHz, $CDCl_3$): δ = 8.56 (s, 1H), 8.03 (d, 1H, *J* = 4.0 Hz), 7.96 (d, 1H, *J* = 8.0 Hz), 7.89 (d, 1H, *J* = 8.0 Hz). 7.48 (d, 1H, *J* = 8.0 Hz), 7.41 (t, 1H, *J* = 8.0 Hz), 7.35 (t, 1H, *J* = 8.0 Hz), 7.28–7.24 (m, 2H), 7.15–7.12 (m, 2H), 6.05 (s, 2H), 3.81 (s, 3H), 3.40 (s, 3H), LRMS (ESI-TOF) *m/z* calcd for $C_{22}H_{19}$ BO_4Na^+ $[M + Na]^+$: 381.13, Found: 381.13.

(*S*)-(2,2'-Dimethoxy-[1,1'-binaphthalen]-3-yl)boronic acid [(*S*)-6]: according to the synthesis path and the method described of (*R*)-**6** above, (*S*)-**6** (0.97 g, 17%) was obtained from (*S*)-**5** (5.00 g, 15.92 mmol). ^{1}H NMR (600 MHz, $CDCl_3$): δ = 8.56 (s, 1H), 8.04 (d, 1H, *J* = 6.0 Hz), 7.96 (d, 1H, *J* = 12.0 Hz), 7.89 (d, 1H, *J* = 6.0 Hz). 7.48 (d, 1H, *J* = 12.0 Hz), 7.41 (t, 1H, *J* = 6.0 Hz), 7.35 (t, 1H, *J* = 12.0 Hz), 7.28–7.24 (m, 2H), 7.15–7.12 (m, 2H), 3.81 (s, 3H), 3.41 (s, 3H), LRMS (ESI-TOF) *m/z* calcd for $C_{22}H_{19}BO_4Na^+$ $[M + Na]^+$: 381.13, Found: 381.13.

(*R*)-(2,2'-Dimethoxy-[1,1'-binaphthalen]-3-yl)trifluoro-λ⁴-borane, potassium salt [(*R*)-7]

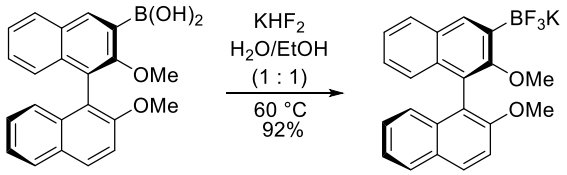

(*R*)-**6** (*R*)-**7**

To a suspension of (*R*)-**6** (0.97 g, 2.71 mmol) in a mixture of water and ethanol (15 mL : 15 mL), potassium hydrogen fluoride (0.85 g, 10.90 mmol) was added. The mixture was stirred at 60 °C for 2 h. The solvent was removed under reduced pressure. The residue was washed with water (60 mL) for 2 h, filtered. (*R*)-**7** (1.05 g, 92%) was obtained as a pale yellow powder, which was employed without further purification. m.p. = 256–261 °C. HRMS (ESI-TOF) *m/z* calcd for $C_{22}H_{17}BF_3O_2^-$ $[M - K]^-$: 381.1274, Found: 381.1312.

(*S*)-(2,2'-Dimethoxy-[1,1'-binaphthalen]-3-yl)trifluoro-λ⁴-borane, potassium salt [(*S*)-7]: according to the synthesis path and the method described of (*R*)-**7** above, (*S*)-**7** (1.05 g, 92%) was obtained from (*S*)-**6** (0.97 g, 2.71 mmol) as a pale yellow powder. m.p. = 256–261 °C. HRMS (ESI-TOF) *m/z* calcd for $C_{22}H_{17}BF_3O_2^-$ $[M - K]^-$: 381.1274, Found: 381.1309.

2,5-Dibromoterephthalic acid (10)

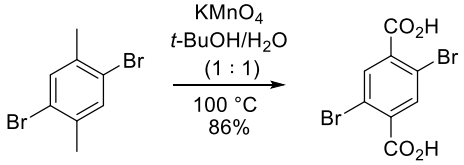

9 **10**

To a solution of 1,4-dibromo-2,5-dimethyl benzene (**9**, 5.00 g, 18.94 mmol) in a mixture of *tert*-butyl alcohol and water (75 mL : 75 mL), potassium permanganate (6.00 g, 37.97 mmol) was added. The reaction mixture was refluxed for 2 h, then an additional portion of potassium permanganate (6.00 g, 37.97 mmol) was added and the reaction was heated under refluxing conditions for 22 h. After the completion of the reaction when the purple disappeared, the mixture was allowed to cool to room temperature. *Tert*-butanol was removed under reduced pressure, then, hydrochloric acid (12 M, 30 mL) was added. The resulting precipitate was collected. The crude product was purified by recrystallization with hot ethanol to afford compound **10** (5.30 g, 86%) as a white powder. ^{1}H NMR (600 MHz, DMSO-d_6): δ = 13.95 (s, 2H), 8.01 (s, 2H), LRMS (ESI-TOF) *m/z* calcd for $C_8H_4Br_2KO_4^+$ $[M + K]^+$: 360.81, Found: 360.81.

Di-*tert*-butyl (2,5-dibromo-1,4-phenylene)dicarbamate (11)

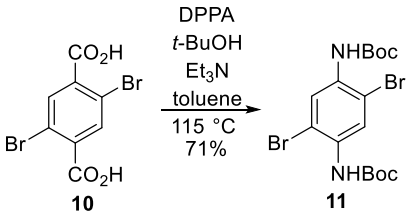

To a mixture of toluene (70 mL), *tert*-butanol (70 mL), triethylamine (5.00 g, 49.50 mmol) and compound **10** (5.30 g, 16.36 mmol), diphenyl azide phosphate (13.60 g, 49.45 mmol) was added. The mixture was heated to reflux for 12 h under nitrogen, then cooled to room temperature and concentrated under reduced pressure. The crude product was purified by recrystallization with ethyl acetate to afford compound **11** (5.40 g, 71%) as a white powder [3]. ^{1}H NMR (600 MHz, $CDCl_3$): δ = 8.38 (s, 2H), 6.88 (s, 2H), 1.53 (s, 18H). LRMS (ESI-TOF) *m/z* [M + Na]$^+$ calcd for $C_{16}H_{22}Br_2NaN_2O_4^+$: 486.98, Found: 486.99.

Di-*tert*-butyl (2,5-divinyl-1,4-phenylene)dicarbamate (12)

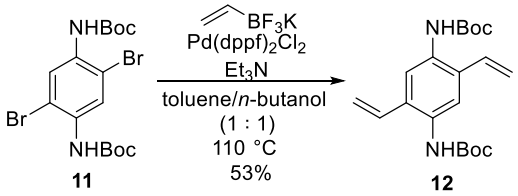

To a solution of toluene (70 mL), *n*-butanol (70 mL) and triethylamine (3.85 g, 38.11 mmol), potassium vinyltrifluoroborate (5.10 g, 38.06 mmol), palladium dichloride [1,1-bis(diphenylphosphino)ferrocene] (1.88 g, 2.30 mmol) and compound **11** (5.40 g, 11.59 mmol) was added. The mixture was heated to 80 °C for 22 h, then cooled to room temperature and concentrated under reduced pressure.[3] Flash chromatography of the residual through silica gel (petroleum ether : dichloromethane = 4 : 1, R_f = 0.2) and then recrystallized by cold dichloromethane afforded compound **12** (2.20 g, 53%) as a pale brown powder. ^{1}H NMR (600 MHz, $CDCl_3$): δ = 7.83 (s, 2H), 6.76 (dd, 2H, *J* = 24.0, 12.0 Hz), 6.33 (s, 2H), 5.72 (d, 2H, *J* = 24.0 Hz), 5.41(d, 2H, *J* = 12.0 Hz), 1.52 (s, 18H). LRMS (ESI-TOF) *m/z* [M + Na]$^+$ calcd for $C_{20}H_{28}NaN_2O_4^+$: 383.19, Found: 383.20.

2,5-Divinylbenzene-1,4-diamine (8)

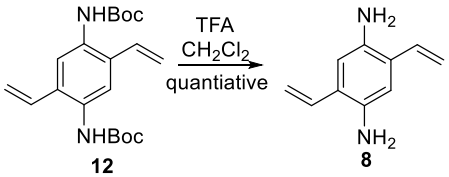

To a suspension of compound **12** (1.60 g, 4.44 mmol) in dichloromethane (20 mL), trifluoroacetic acid (5 mL) was added. The mixture was stirred for 4 h and then concentrated under reduced pressure. The residual was washed with sodium carbonate (saturated solution) and then extracted with ethyl acetate (30 mL × 3). The combined organic phase was concentrated under reduced pressure[3]. The compound **8** (0.71 g, equivalent) was obtained as a yellow solid which was

employed without further purification.

2,7-Bis((*R*)-2,2'-dimethoxy-[1,1'-binaphthalen]-3-yl)-1,2,6,7-tetrahydrobenzo[1,2-e:4,5-e']bis([1,2]azaborinine) [(*R*,*R*)-DBM-BNA][(*R*,*R*)-1]

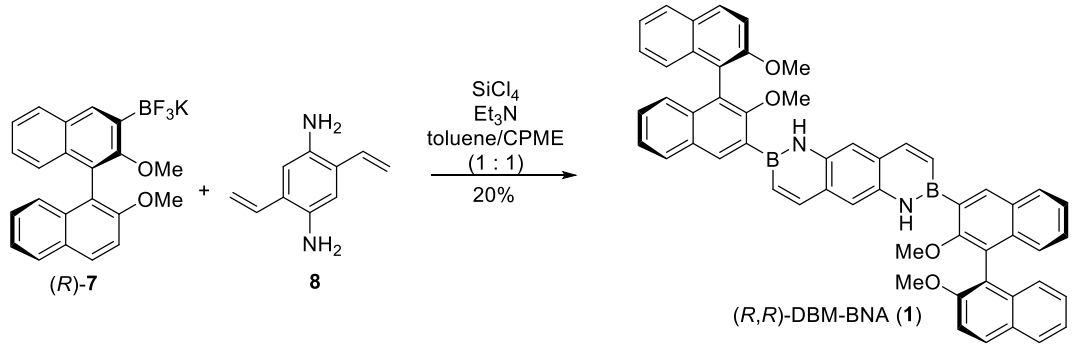

To a mixture of (*R*)-**7** (4.40 g, 10.48 mmol) and compound **8** (0.71 g, 4.44 mmol) in toluene (75 mL) and cyclopentyl methyl ether (75 mL), silicon tetrachloride (1.80 g, 10.59 mmol) and triethylamine (4.40 g, 43.56 mmol) were injected under nitrogen. The mixture was heated to reflux for 12 h. The mixture was concentrated under reduced pressure. Flash chromatography of the residual through silica gel (petroleum ether ： dichloromethane = 3 ： 1; R_f = 0.1) afforded (*R*,*R*)-DBM-BNA (**1**) (0.71 g, 20%) as a yellow powder. m.p. > 350°C. ^{1}H NMR (600 MHz, CD_2Cl_2): δ = 9.60 (s, 2H), 8.67 (s, 2H), 8.25 (d, 2H, *J* = 12.0 Hz), 8.09 (d, 2H, *J* = 6.0 Hz), 8.03 (d, 2H, *J* = 6.0 Hz), 7.94 (d, 2H, *J* = 6.0 Hz), 7.60 (s, 2H), 7.55 (m, 4H), 7.43 (t, 2H, *J* = 6.0 Hz), 7.36 (t, 2H, *J* = 6.0 Hz), 7.29–7.25 (m, 4H), 7.18 (d, 2H, *J* = 12.0 Hz), 7.13 (d, 2H, *J* = 6.0 Hz), 3.85 (s, 6H), 3.50 (s, 6H); ^{13}C{^{1}H} NMR (100 MHz, $CDCl_3$): δ = 160.8, 155.3, 144.8, 138.7, 135.5, 135.4, 134.5, 131.4, 130.1, 129.5, 129.0, 128.4, 127.3, 127.1, 126.9, 125.6, 125.5, 125.2, 125.1, 124.0, 119.5, 117.2, 113.7, 61.6, 56.6. Two carbon resonances was not recognized due to peak overlapping. HRMS (ESI-TOF) *m/z* calcd for $C_{54}H_{43}B_2N_2O_4^+$ $[M + H]^+$: 805.3403, Found: 805.3393.

2,7-Bis((*S*)-2,2'-dimethoxy-[1,1'-binaphthalen]-3-yl)-1,2,6,7-tetrahydrobenzo[1,2-e:4,5-e']bis([1,2]azaborinine) [(*S*,*S*)-DBM-BNA] [(*S*,*S*)-1]: according to the synthesis path and the method described of (*R*,*R*)-**1** above, (*S*,*S*)-**1** (0.85 g, 24%) was obtained from **8** (0.71 g, 4.44 mmol) as a yellow powder. m.p. > 350 °C. ^{1}H NMR (600 MHz, CD_2Cl_2): δ = 9.60 (s, 2H), 8.67 (s, 2H), 8.25 (d, 2H, *J* = 12.0 Hz), 8.09 (d, 2H, *J* = 6.0 Hz), 8.03 (d, 2H, *J* = 6.0 Hz), 7.94 (d, 2H, *J* = 6.0 Hz), 7.62 (s, 2H), 7.58–7.55 (m, 4H), 7.43 (t, 2H, *J* = 6.0 Hz), 7.36 (t, 2H, *J* = 6.0 Hz), 7.29–7.25 (m, 4H), 7.18 (d, 2H, *J* = 12.0 Hz), 7.13 (d, 2H, *J* = 6.0 Hz), 3.85 (s, 6H), 3.50 (s, 6H); ^{13}C{^{1}H} NMR (125 MHz, CD_2Cl_2): δ = 160.8, 155.3, 144.8, 138.7, 135.5, 135.4, 130.1, 129.5, 129.0, 128.4, 127.3, 127.1, 126.9, 125.6, 125.5, 125.2, 124.0, 119.6, 118.3, 117.2, 113.7, 61.6, 56.6. Four carbon resonances was not recognized due to peak overlapping. HRMS (ESI-TOF) *m/z* calcd for $C_{54}H_{42}B_2N_2O_4Na^+$ $[M + Na]^+$: 827.3228, Found: 827.3209.

(1*R*,1''*R*)-3,3''-(1,6-Dihydrobenzo[1,2-e:4,5-e']bis([1,2]azaborinine)-2,7-diyl)bis([1,1'-binaphthalene]-2,2'-diol) [(*R*,*R*)-DBH-BNA] [(*R*,*R*)-2]

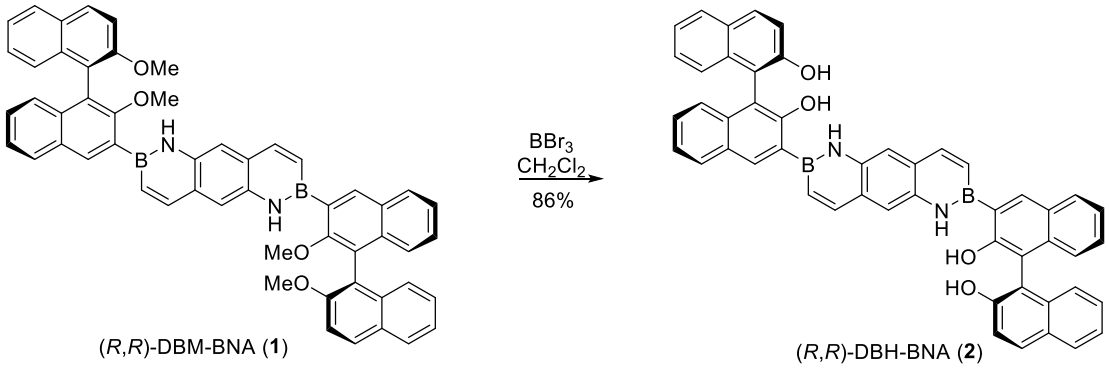

(*R*,*R*)-DBM-BNA (**1**) (*R*,*R*)-DBH-BNA (**2**)

To a mixture of (*R*,*R*)-DBM-BNA (**1**) (0.10 g, 0.12 mmol) in dichloromethane (10 mL), boron tribromide (1 M in dichloromethane, 0.3 mL, 0.3 mmol) was added. The reaction mixture was stirred at room temperature for 2 h. Water (10 mL) was added to quench the reaction. The mixture was concentrated under reduced pressure. Flash chromatography of the residual through silica gel (petroleum ether： ethyl acetate = 3 ： 1; R_f = 0.2) afforded (*R*,*R*)-DBH-BNA (**2**) (0.08 g, 86%) as a pale yellow powder. m.p. > 350 °C. ^{1}H NMR (600 MHz, DMSO-d_6): δ = 10.34 (s, 2H), 9.48 (s, 2H), 8.58 (s, 2H), 8.33 (s, 2H), 8.27 (d, 2H, *J* = 18.0 Hz), 8.03 (d, 2H, *J* = 12.0 Hz), 7.97 (d, 2H, *J* = 12.0 Hz), 7.94 (d, 2H, *J* = 12.0 Hz), 7.91 (s, 2H), 7.55 (d, 2H, *J* = 18.0 Hz), 7.42 (d, 2H, *J* = 12.0 Hz), 7.32 (q, 4H, *J* = 12.0 Hz), 7.25 (q, 4H, *J* = 12.0 Hz), 7.05 (d, 2H, *J* = 12.0 Hz), 6.91 (d, 2H, *J* = 12.0 Hz); ^{13}C{^{1}H} NMR (125 MHz, DMSO-d_6): δ = 156.3, 154.1, 143.6, 136.6, 134.9, 134.7, 134.5, 130.9, 129.4, 128.5, 128.41, 128.37, 128.0, 127.8, 126.4, 126.1, 126.0, 124.2, 124.1, 122.5, 122.3, 118.8, 116.7, 115.2, 113.6. HRMS (ESI-TOF) *m/z* calcd for $C_{50}H_{34}B_2N_2O_4Na^+$ [M + Na]$^+$: 771.2602, Found: 771.2590.

(1*S*,1''*S*)-3,3''-(1,6-Dihydrobenzo[1,2-e:4,5-e']bis([1,2]azaborinine)-2,7-diyl)bis([1,1'-binaphthalene]-2,2'-diol) [(*S*,*S*)-DBH-BNA] [(*S*,*S*)-2]: according to the synthesis path and the method described of (*R*,*R*)-**2** above, (*S*,*S*)-**2** (0.08 g, 86%) was obtained from (*S*,*S*)-**1** (0.10 g, 0.12 mmol) as a pale yellow powder. m.p. > 350 °C. ^{1}H NMR (600 MHz, DMSO-d_6): δ = 10.35 (s, 2H), 9.49 (s, 2H), 8.58 (s, 2H), 8.34 (s, 2H), 8.27 (d, 2H, *J* = 12.0 Hz), 8.03 (d, 2H, *J* = 6.0 Hz), 7.97 (d, 2H, *J* = 12.0 Hz), 7.94 (d, 2H, *J* = 6.0 Hz), 7.91 (s, 2H), 7.54 (d, 2H, *J* = 12.0 Hz), 7.42 (d, 2H, *J* = 12.0 Hz), 7.32 (q, 4H, *J* = 6.0 Hz), 7.25 (q, 4H, *J* = 6.0 Hz), 7.05 (d, 2H, *J* = 6.0 Hz), 6.91 (d, 2H, *J* = 6.0 Hz); ^{13}C{^{1}H} NMR (125 MHz, DMSO-d_6): δ = 156.3, 154.1, 143.7, 136.6, 134.9, 134.7, 134.5, 131.0, 129.5, 128.5, 128.4, 128.0, 126.5, 126.13, 126.09, 124.3, 124.2, 122.5, 122.4, 118.8, 116.7, 115.2, 113.6. Two carbon resonances were not recognized due to peak overlapping. HRMS (ESI-TOF) *m/z* calcd for $C_{50}H_{34}B_2N_2O_4Na^+$ [M + Na]$^+$: 771.2602, Found: 771.2596.

(11c*R*,11c'*R*)-2,2'-(1,6-Dihydrobenzo[1,2-e:4,5-e']bis([1,2]azaborinine)-2,7-diyl)bis(4-hydroxydinaphtho[2,1-*d*:1',2'-*f*][1,3,2]dioxaphosphepine 4-oxide) [(*R*,*R*)-DBP-BNA] [(*R*,*R*)-3]

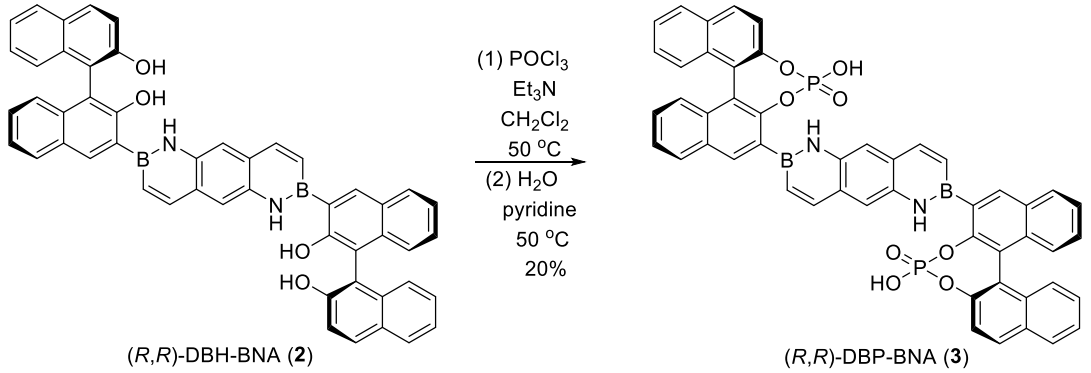

(*R*,*R*)-DBH-BNA (**2**) (*R*,*R*)-DBP-BNA (**3**)

To a solution of (*R*,*R*)-DBH-BNA (**2**) (0.08 g, 0.11 mmol) in dichloromethane (15 mL), phosphorus oxychloride (0.17 g, 1.1 mmol) and triethylamine (0.23 g, 2.16 mmol) were added. The temperature of the mixture was raised up to 40 °C for 12 h. The mixture was concentrated under reduced pressure. Then pyridine (15 mL) and water (3 mL) were added to the residue and the temperature was raised up to 50 °C for 2 h. The mixture was concentrated under reduced pressure. Flash chromatography of the residual through silica gel (ethanol ： dichloromethane = 1 ： 9; R_f = 0.1) afforded (*R*,*R*)-DBP-BNA (**3**) (0.02 g, 20%) as a yellow powder. m.p. > 350 °C. ^{1}H NMR (600 MHz, DMSO-d_6): δ = 12.06 (s, 2H), 8.47 (s, 2H), 8.41 (d, 2H, *J* = 12.0 Hz), 8.15 (d, 4H, *J* = 6.0 Hz), 8.09 (d, 2H, *J* = 12.0 Hz), 7.90 (s, 2H), 7.61 (d, 2H, *J* = 6.0 Hz), 7.50 (t, 4H, *J* = 6.0 Hz), 7.42 (d, 2H, *J* = 12.0 Hz), 7.35 (t, 4H, *J* = 12.0 Hz), 7.27 (d, 2H, *J* = 6.0 Hz), 7.21 (d, 2H, *J* = 6.0 Hz); ^{13}C{^{1}H} NMR (125 MHz, DMSO-d_6): δ = 152.2, 149.7, 144.4, 137.5, 135.1, 133.3, 132.6, 132.1, 131.3, 130.6, 130.3, 129.9, 128.7, 128.4, 126.4, 126.3, 126.2, 126.1, 126.0, 124.7, 124.6, 122.7, 122.3, 121.3 116.8. HRMS (ESI-TOF) *m/z* calcd for $C_{50}H_{32}B_2N_2O_8P_2Na^+$ [M + Na]$^+$: 895.1718, Found: 895.1760.

(11c*S*,11c'*S*)-2,2'-(1,6-Dihydrobenzo[1,2-e:4,5-e']bis([1,2]azaborinine)-2,7-diyl)bis(4-hydroxydinaphtho[2,1-d:1',2'-f][1,3,2]dioxaphosphepine 4-oxide) [(*S*,*S*)-DBP-BNA] [(*S*,*S*)-3]: according to the synthesis path and the method described of (*R*,*R*)-**3** above, (*S*,*S*)-**3** (0.02 g, 20%) was obtained from (*S*,*S*)-**2** (0.08 g, 0.11 mmol) as a yellow powder. m.p. > 350 °C. ^{1}H NMR (600 MHz, DMSO-d_6): δ = 12.08 (s, 2H), 8.47 (s, 2H), 8.41 (d, 2H, *J* = 12.0 Hz), 8.15 (d, 4H, *J* = 12.0 Hz), 8.10 (d, 2H, *J* = 6.0 Hz), 7.90 (s, 2H), 7.60 (d, 2H, *J* = 6.0 Hz), 7.50 (t, 4H, *J* = 6.0 Hz), 7.42 (d, 2H, *J* = 12.0 Hz), 7.35 (t, 4H, *J* = 12.0 Hz), 7.27 (d, 2H, *J* = 6.0 Hz), 7.21 (d, 2H, *J* = 6.0 Hz); ^{13}C{^{1}H} NMR (125 MHz, DMSO-d_6): δ = 152.3, 149.6, 144.4, 137.5, 135.1, 133.3, 132.6, 132.1, 131.4, 130.6, 130.3, 129.9, 128.7, 128.4, 126.4, 126.3, 126.2, 126.09, 126.05, 124.7, 124.6, 122.7, 122.3, 121.2, 116.7. HRMS (ESI-TOF) *m/z* calcd for $C_{50}H_{31}B_2N_2O_8P_2^-$ [M – H]$^-$: 871.1742, Found: 871.1768.

3. ^{1}H and ^{13}C NMR spectra

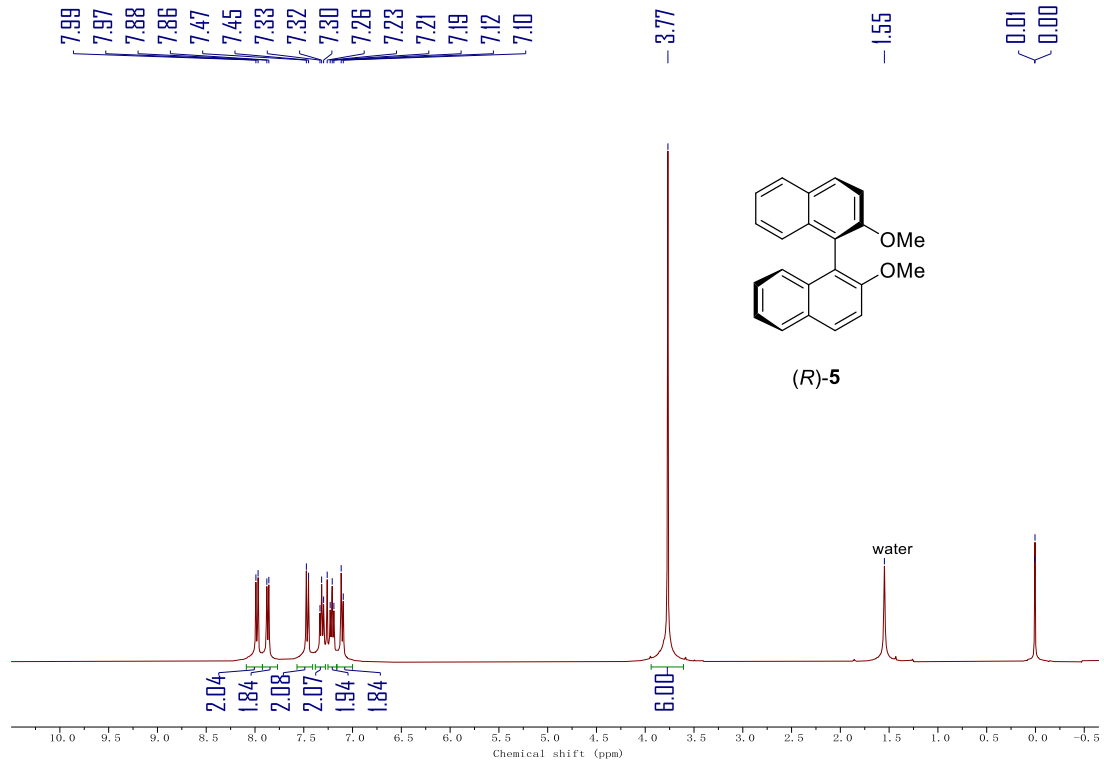

Figure S1. ^{1}H NMR spectrum of (*R*)-**5** ($CDCl_3$, 600 MHz, 25 °C).

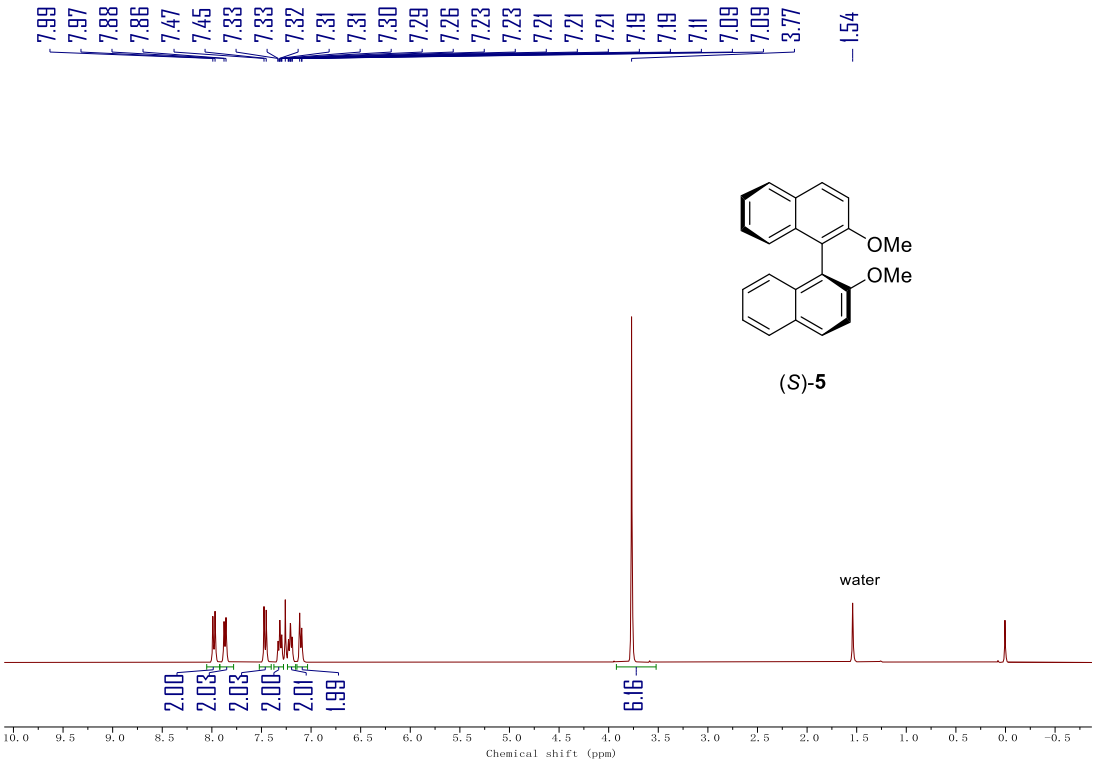

Figure S2. ^{1}H NMR spectrum of (*S*)-**5** ($CDCl_3$, 400 MHz, 25 °C).

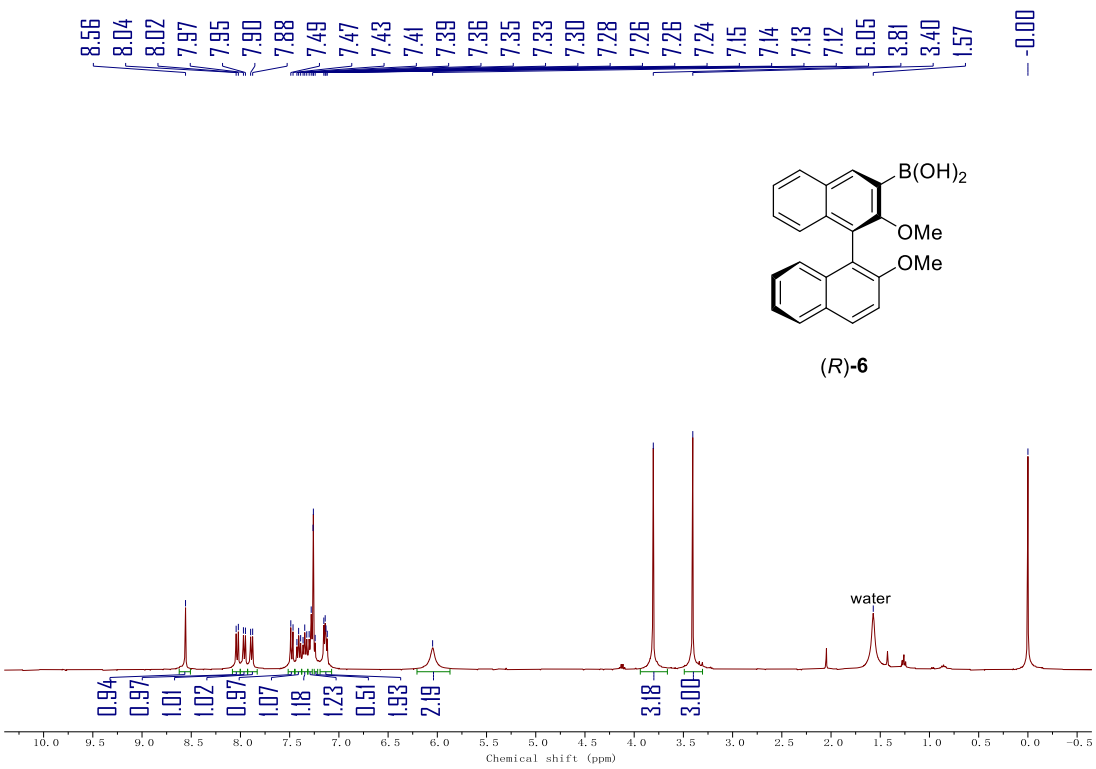

(*R*)-**6**

Figure S3. ^{1}H NMR spectrum of (*R*)-**6** ($CDCl_3$, 400 MHz, 25 °C).

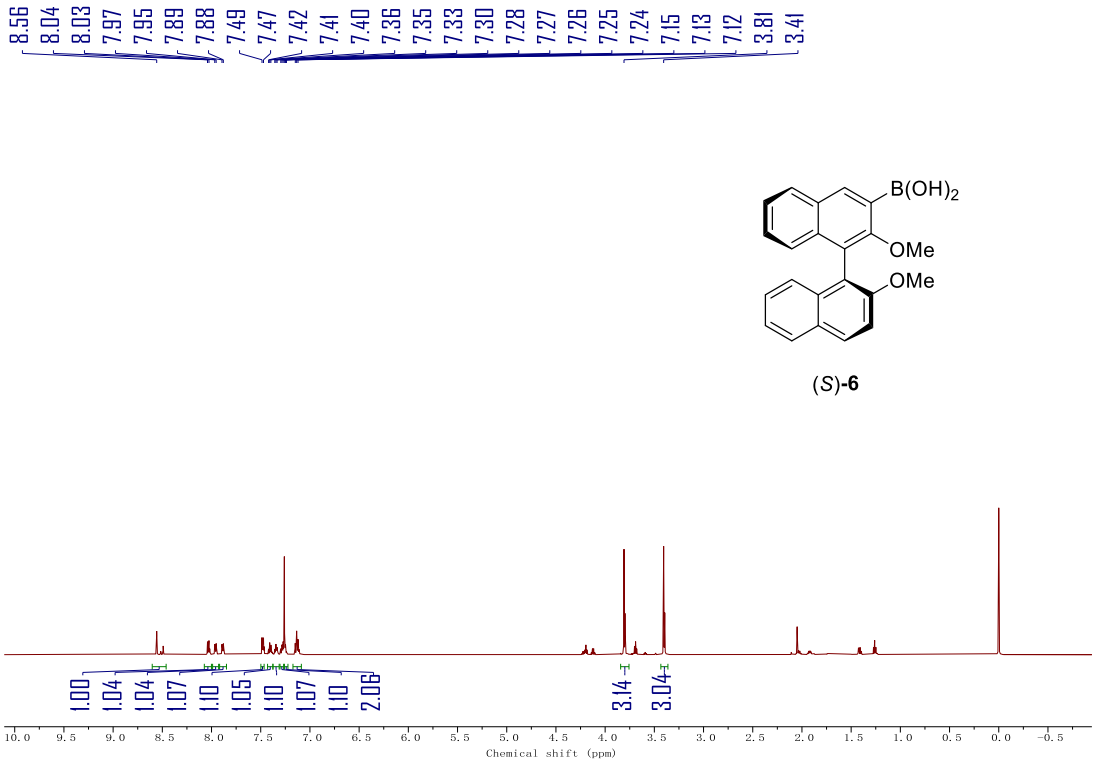

(*S*)-**6**

Figure S4. ^{1}H NMR spectrum of (*S*)-**6** ($CDCl_3$, 600 MHz, 25 °C).

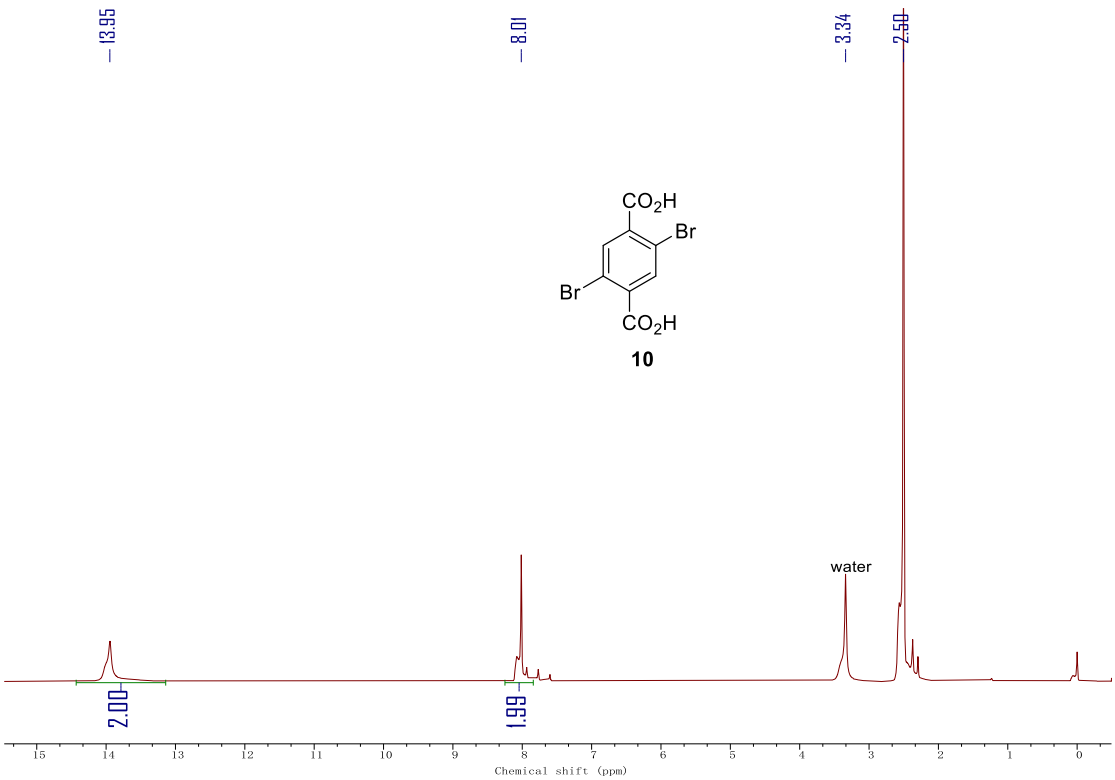

Figure S5. ^{1}H NMR spectrum of **10** (DMSO-d_6, 600 MHz, 25 °C).

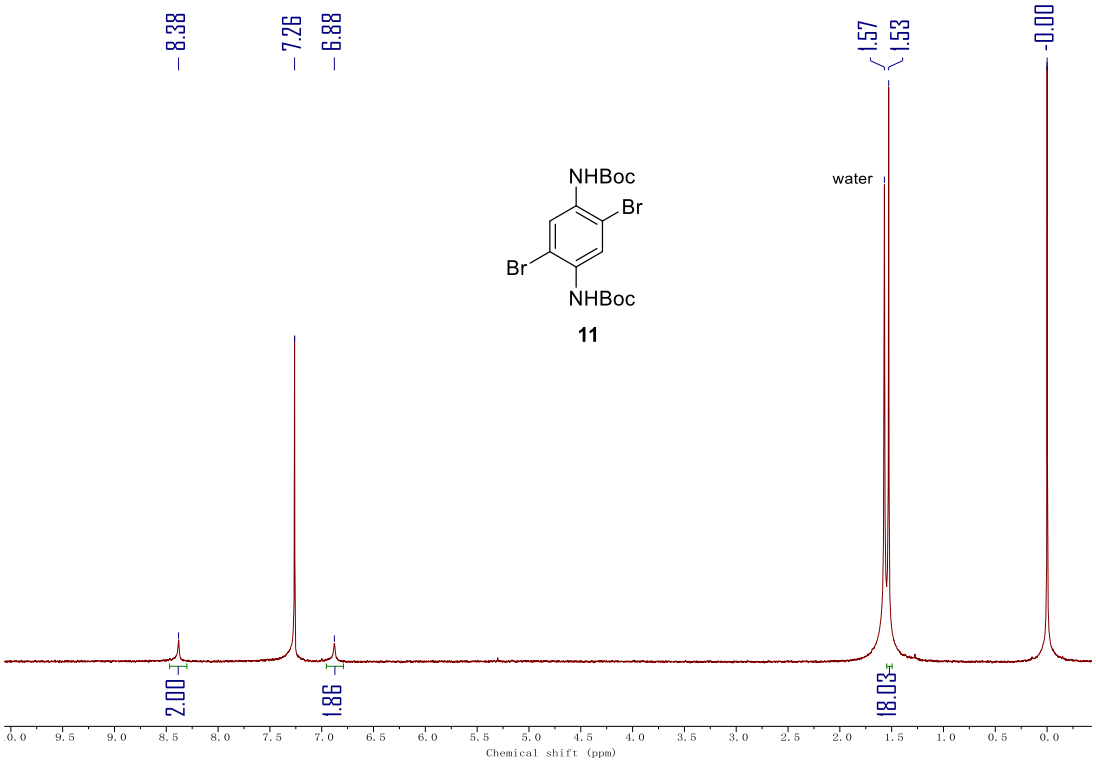

Figure S6. ^{1}H NMR spectrum of **11** ($CDCl_3$, 600 MHz, 25 °C).

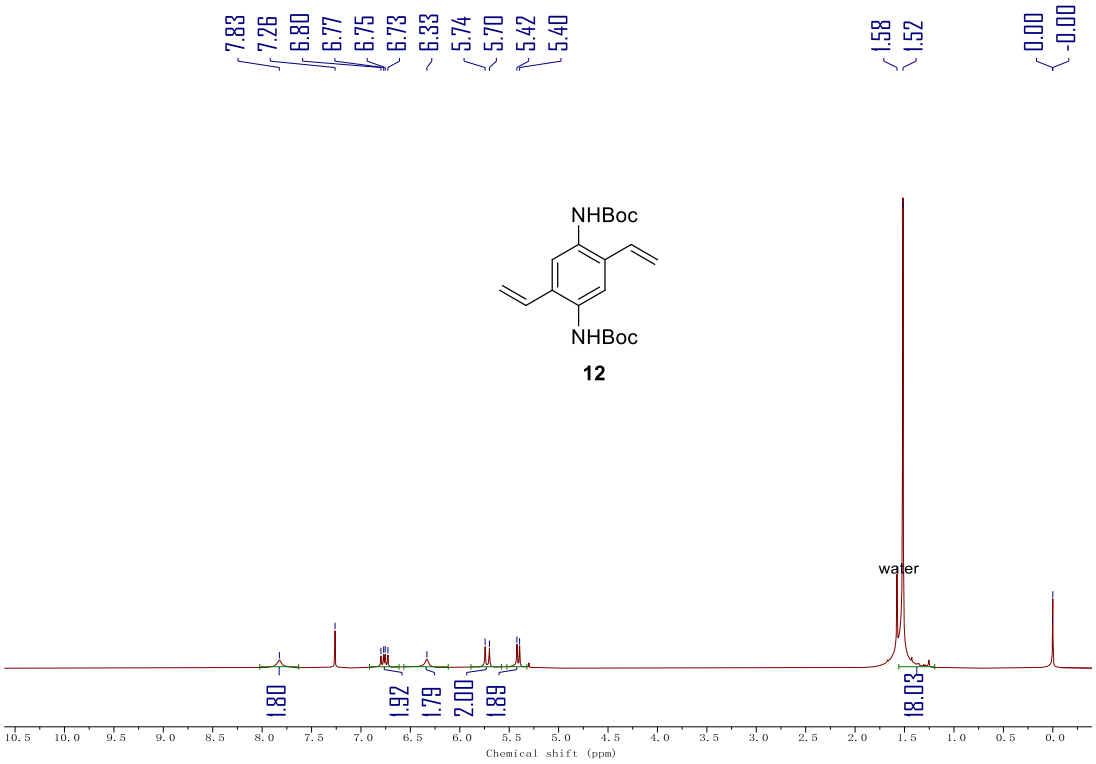

Figure S7. ^{1}H NMR spectrum of **12** ($CDCl_3$, 600 MHz, 25 °C).

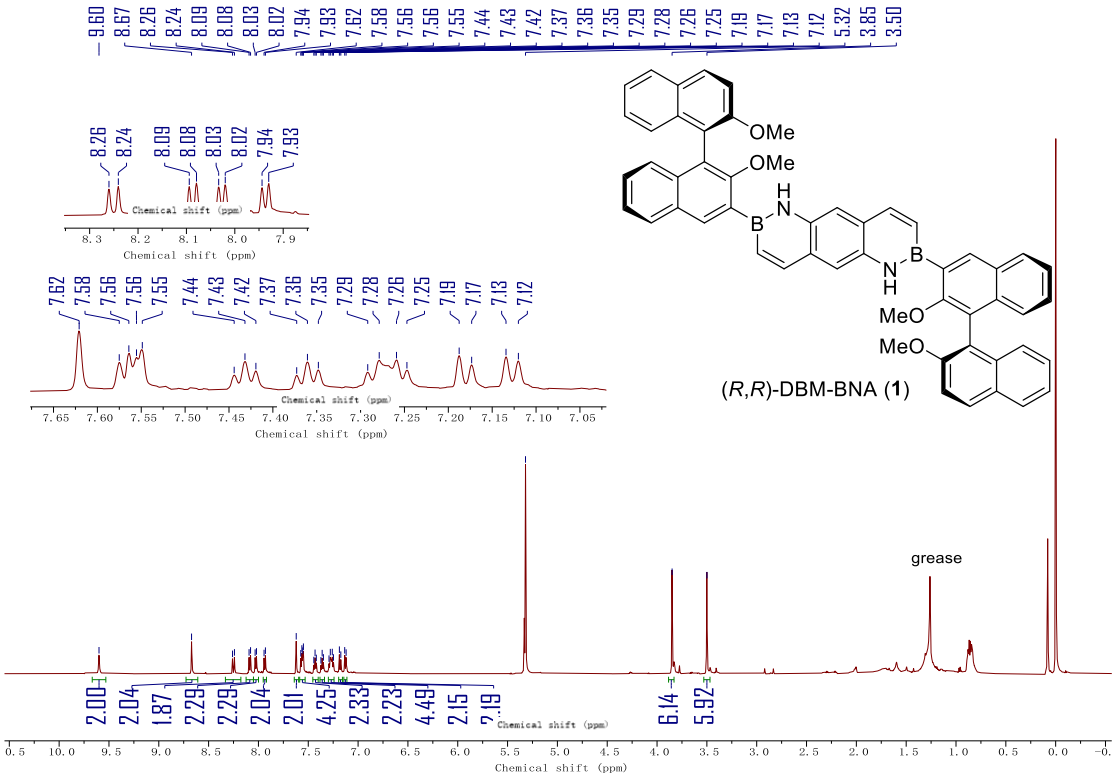

Figure S8. ^{1}H NMR (CD_2Cl_2, 600 MHz, 25 °C) spectrum of (*R*,*R*)-DBM-BNA (**1**).

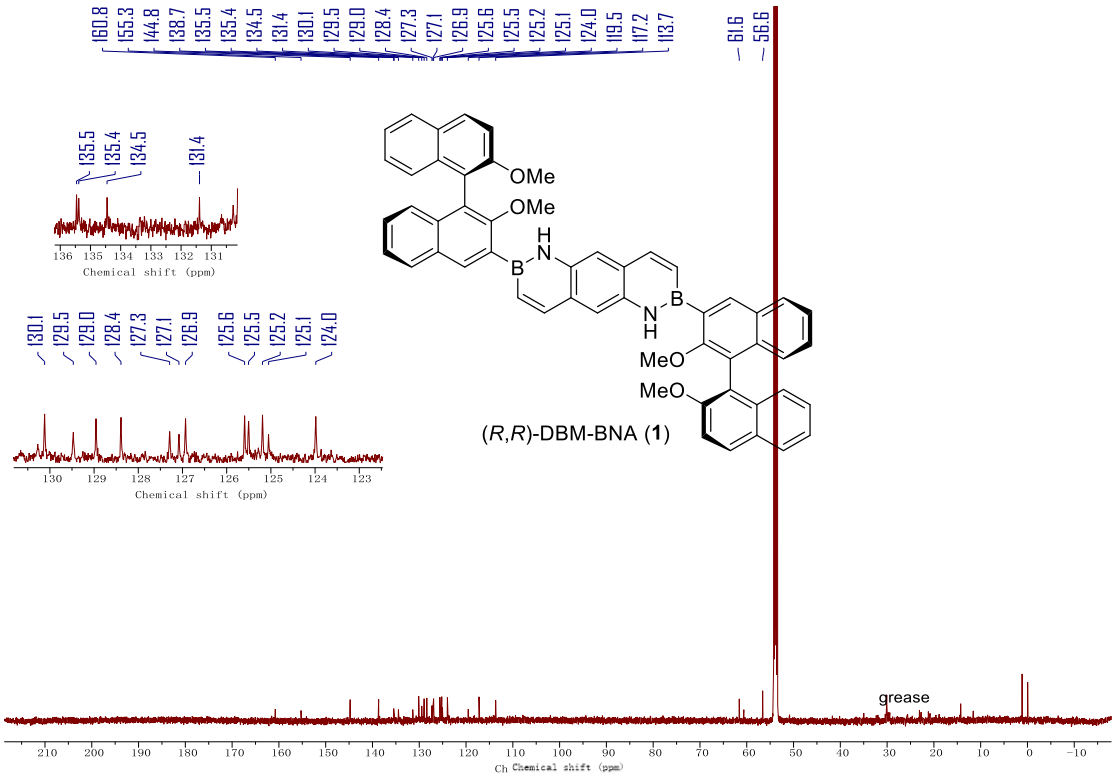

Figure S9. ^{13}C NMR (CD_2Cl_2, 125 MHz, 25 °C) spectrum of (*R*,*R*)-DBM-BNA (**1**).

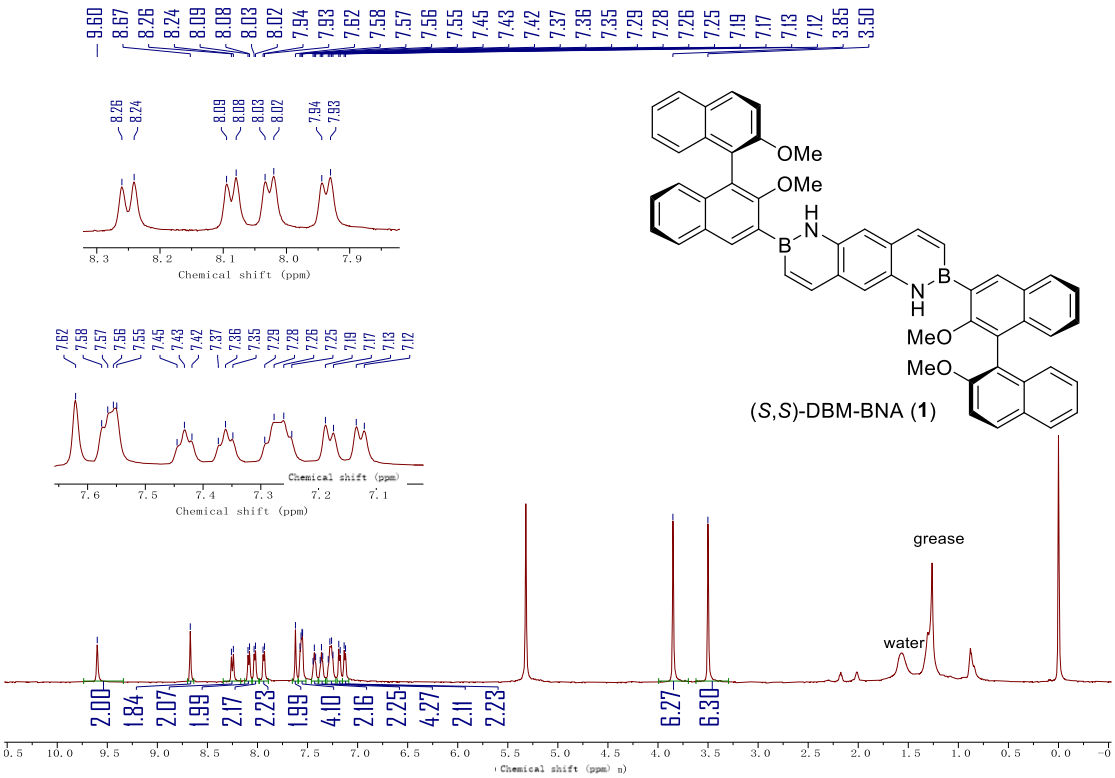

Figure S10. ^{1}H NMR (CD_2Cl_2, 600 MHz, 25 °C) spectrum of (*S*,*S*)-DBM-BNA (**1**).

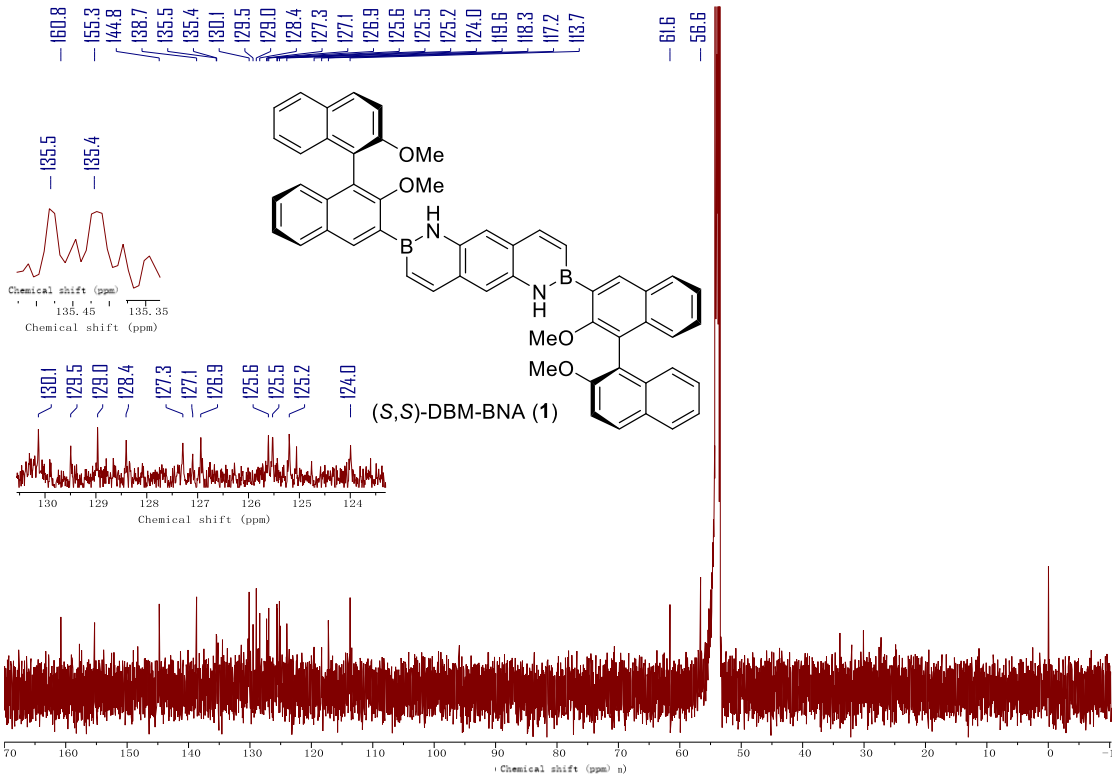

Figure S11. ^{13}C NMR (CD_2Cl_2, 125 MHz, 25 °C) spectrum of (*S*,*S*)-DBM-BNA (**1**).

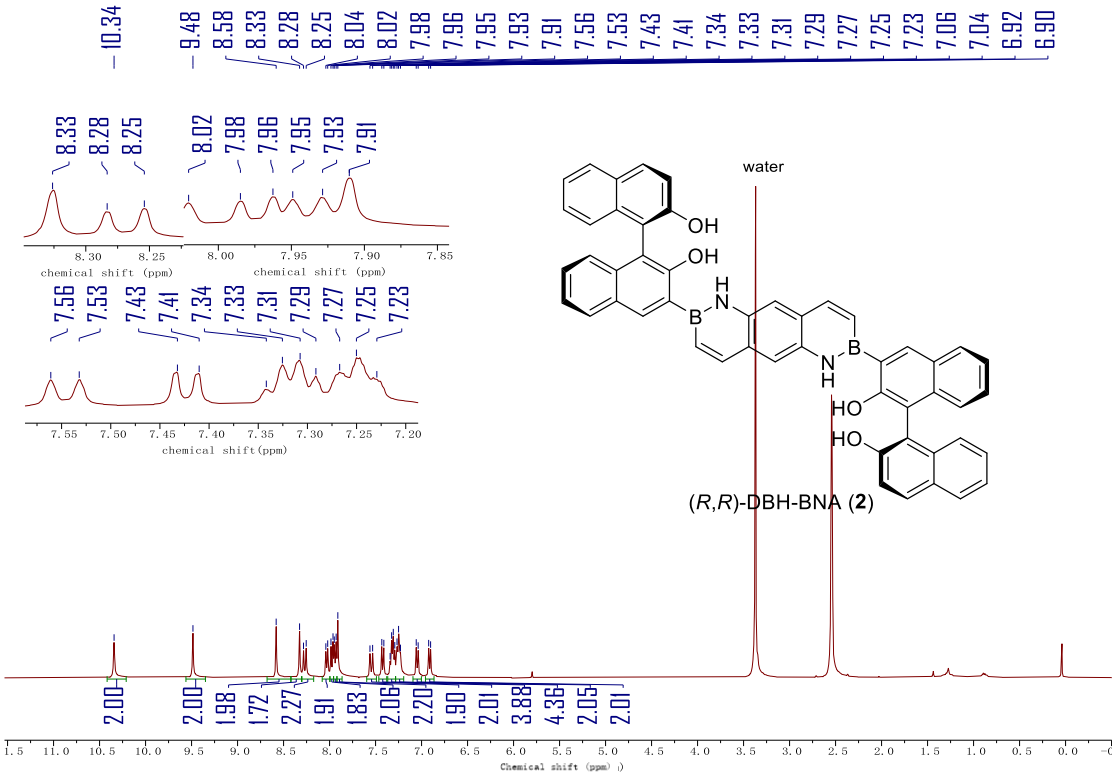

Figure S12. ^{1}H NMR (DMSO-d_6, 600 MHz, 25 °C) spectrum of (*R*,*R*)-DBH-BNA (**2**).

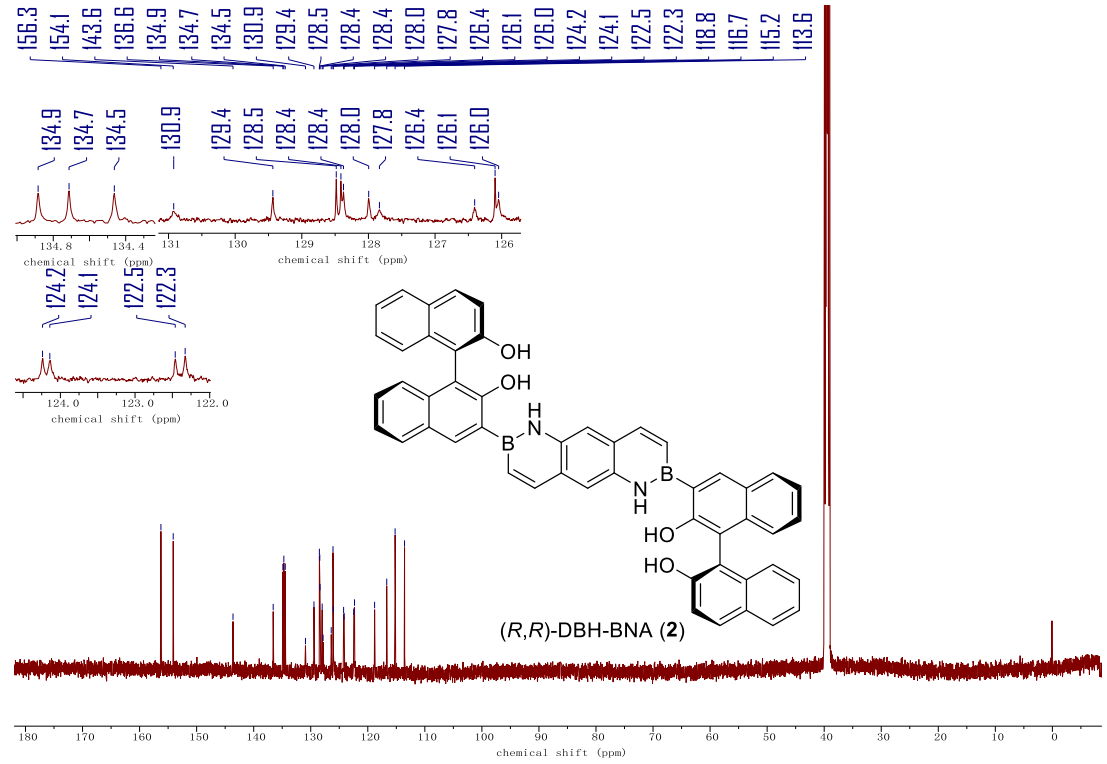

Figure S13. ^{13}C NMR (DMSO-d_6, 125 MHz, 25 °C) spectrum of (*R*,*R*)-DBH-BNA (**2**).

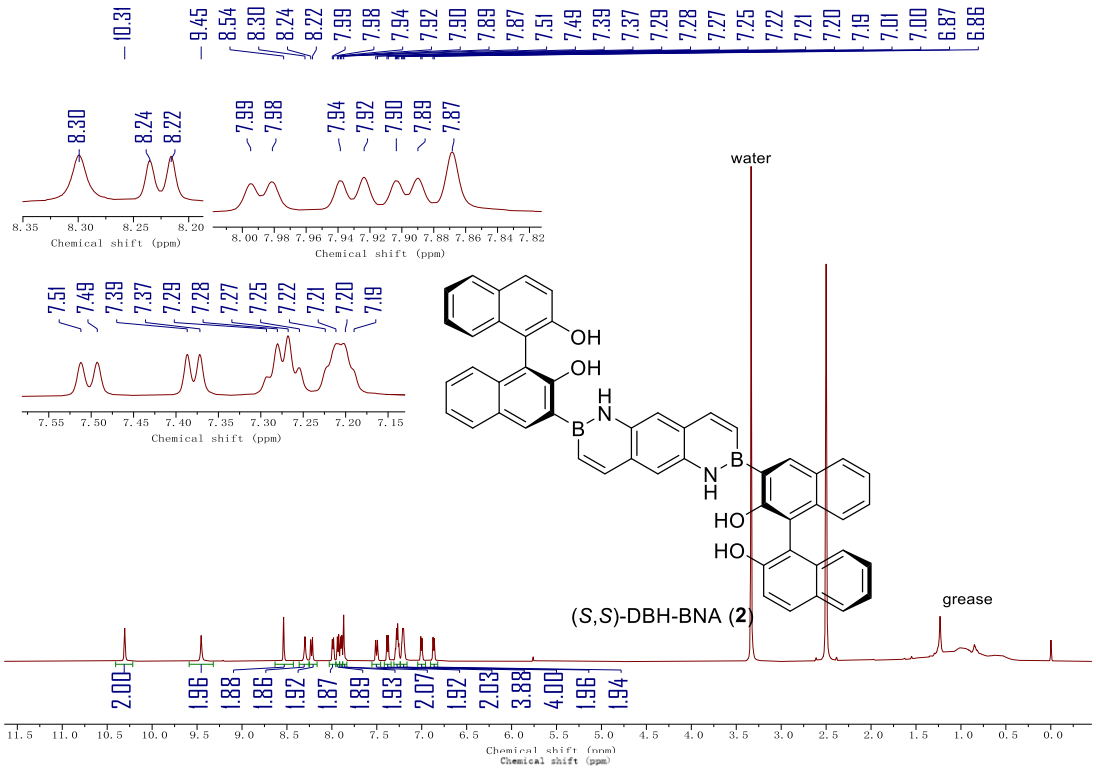

Figure S14. ^{1}H NMR (DMSO-d_6, 600 MHz, 25 °C) spectrum of (*S*,*S*)-DBH-BNA (**2**).

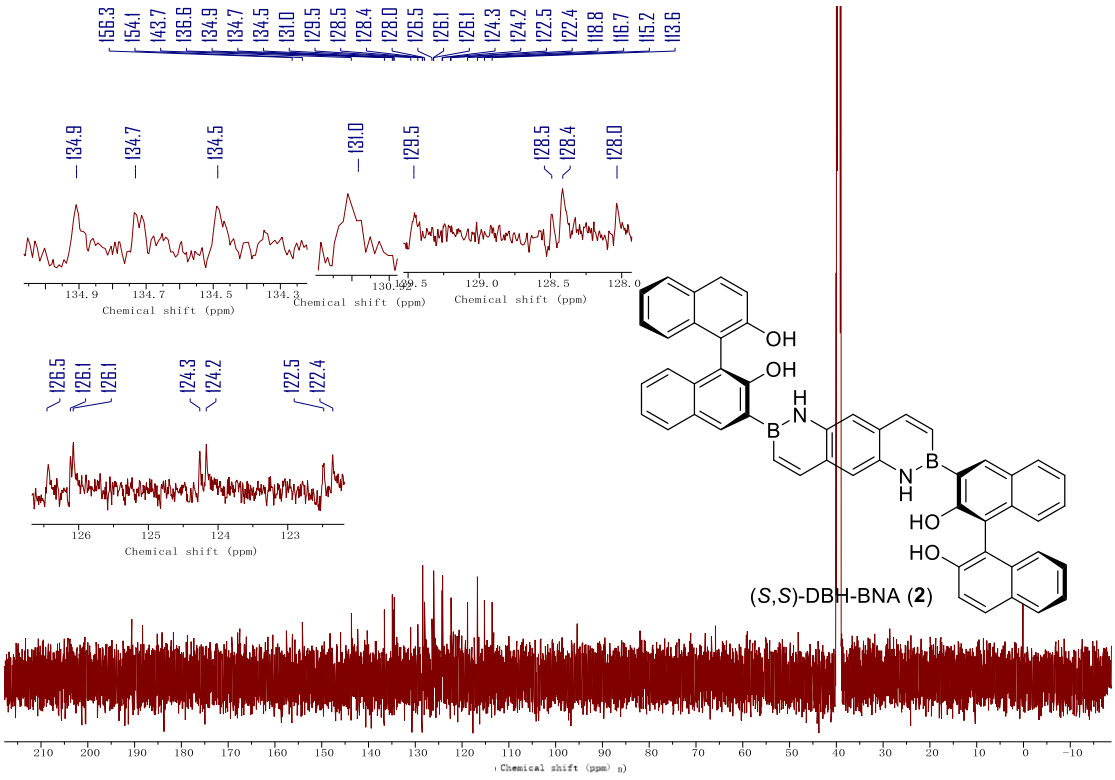

Figure S15. ^{13}C NMR (DMSO-d_6, 125 MHz, 25 °C) spectrum of (*R*,*R*)-DBH-BNA (**2**).

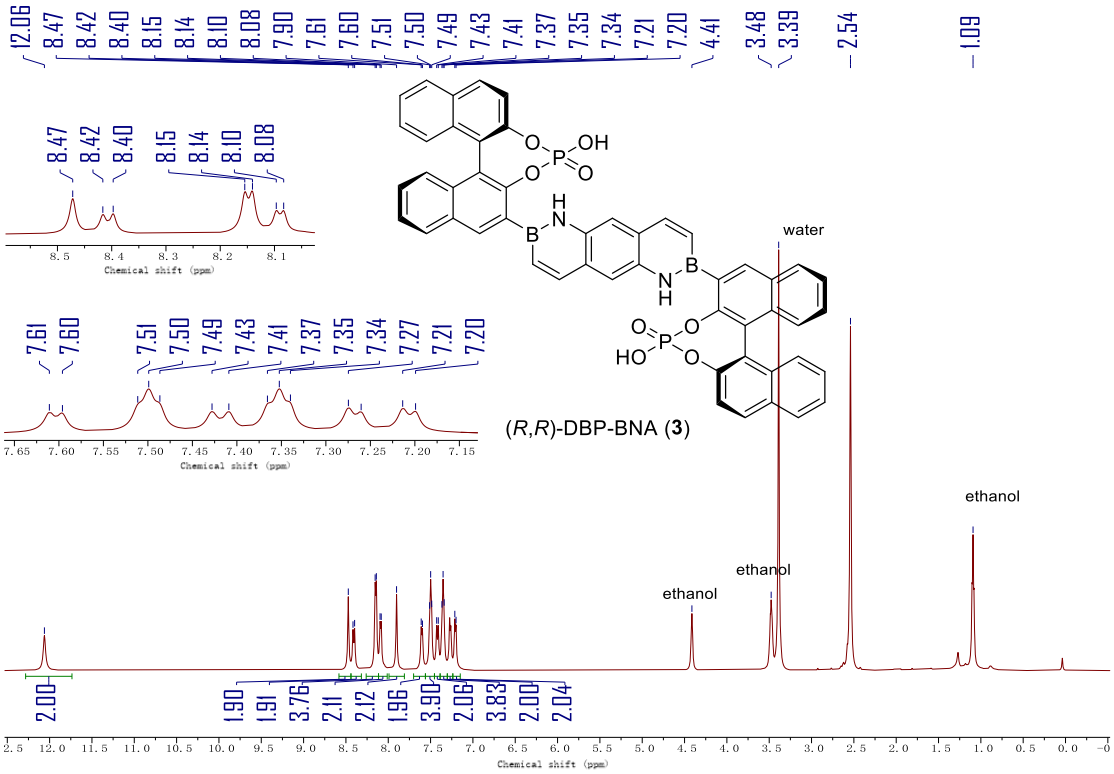

Figure S16. ^{1}H NMR (DMSO-d_6, 600 MHz, 25 °C) spectrum of (*R*,*R*)-DBP-BNA (**3**).

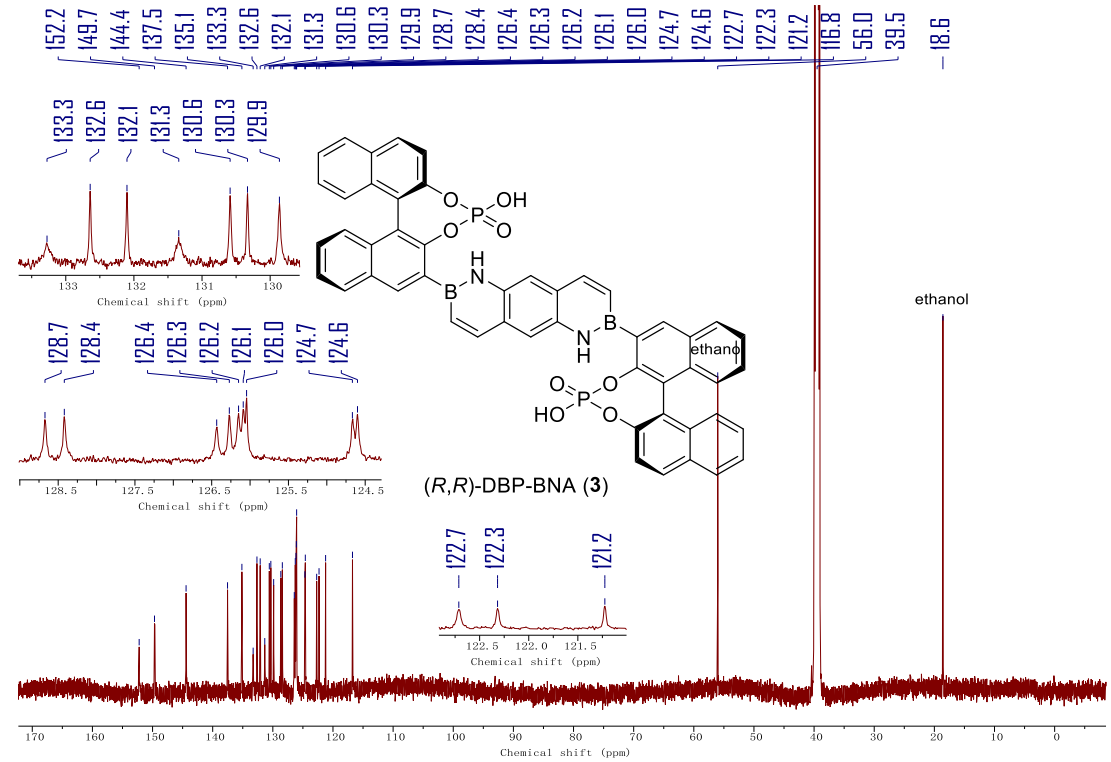

Figure S17. ^{13}C NMR (DMSO-d_6, 125 MHz, 25 °C) spectrum of (*R*,*R*)-DBP-BNA (**3**).

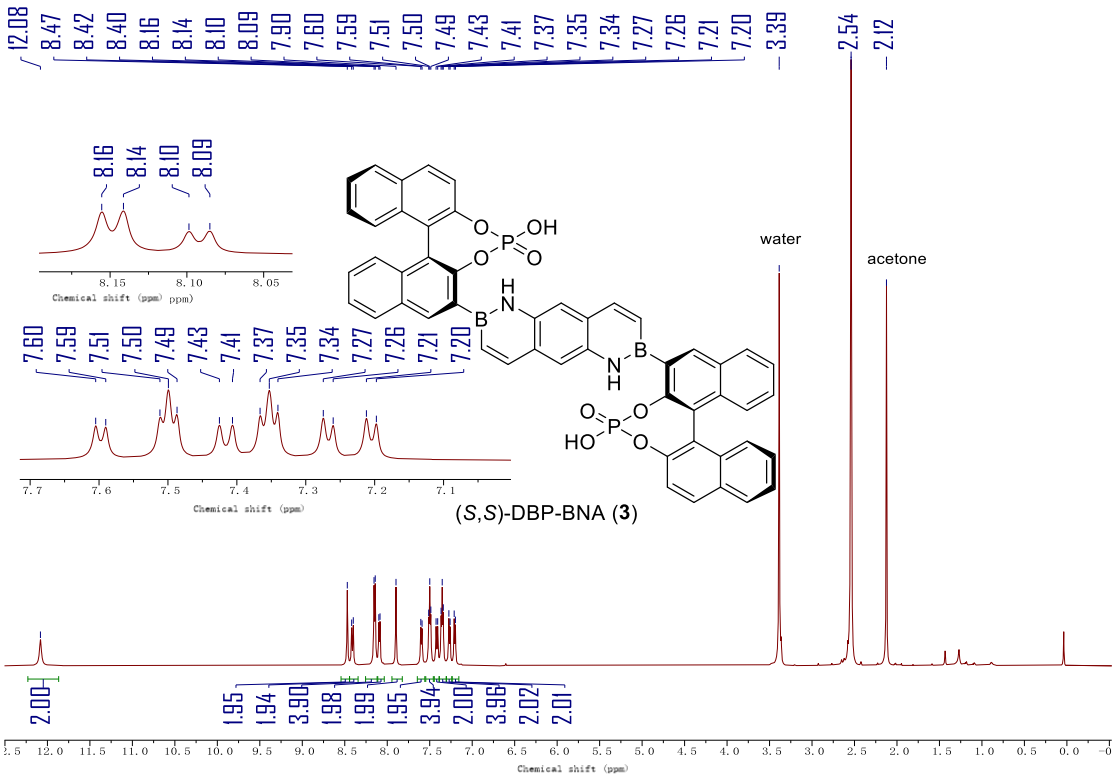

Figure S18. ^{1}H NMR (DMSO-d_6, 600 MHz, 25 °C) spectrum of (*S*,*S*)-DBP-BNA (**3**).

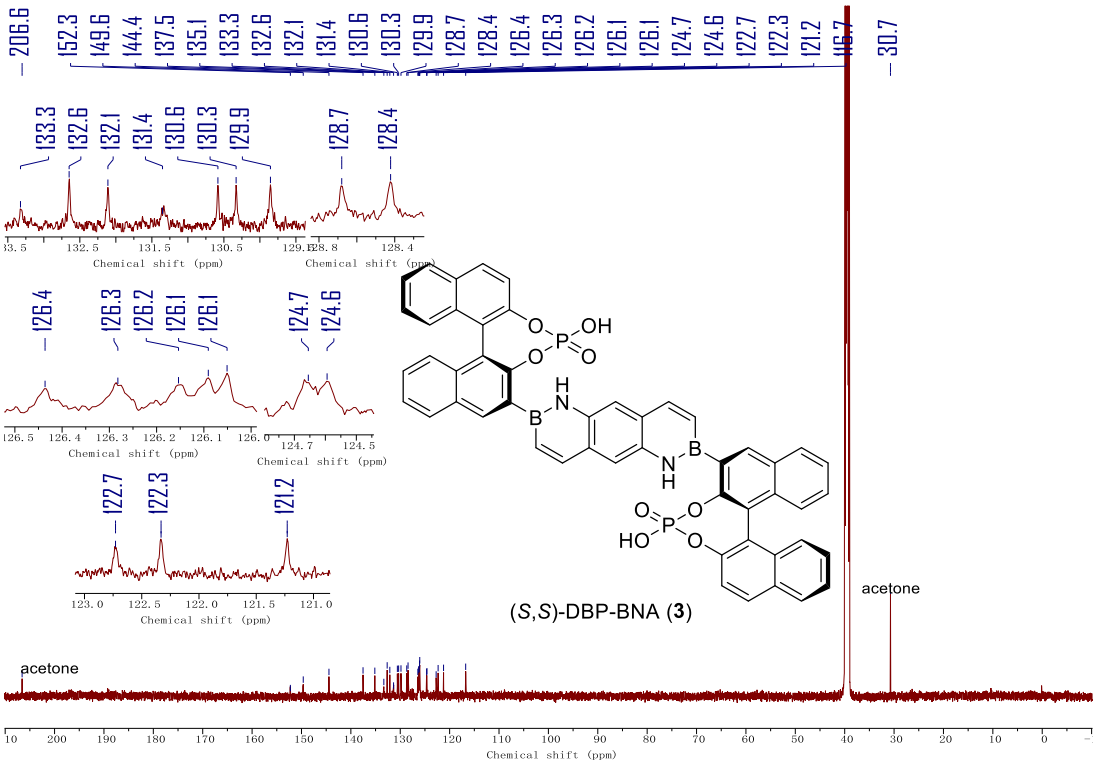

Figure S19. ^{13}C NMR (DMSO-d_6, 125 MHz, 25 °C) spectrum of (*S*,*S*)-DBP-BNA (**3**).

4. Mass spectrum

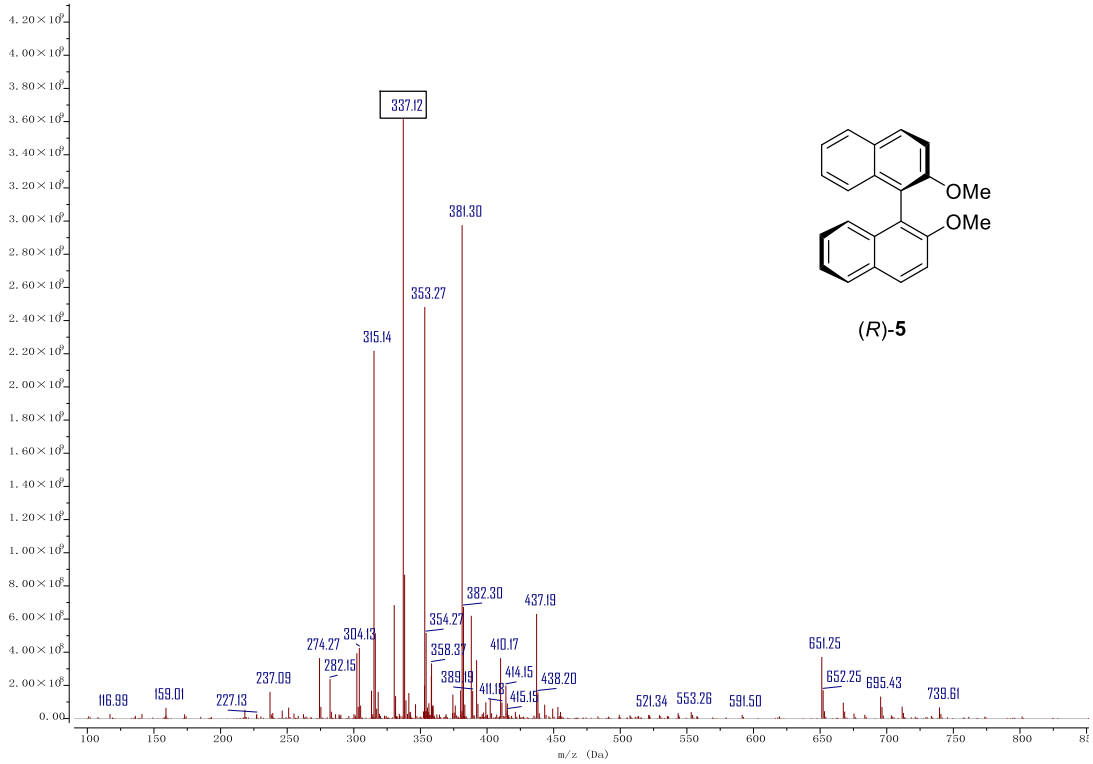

Figure S20. LRMS spectrum of (*R*)-**5**.

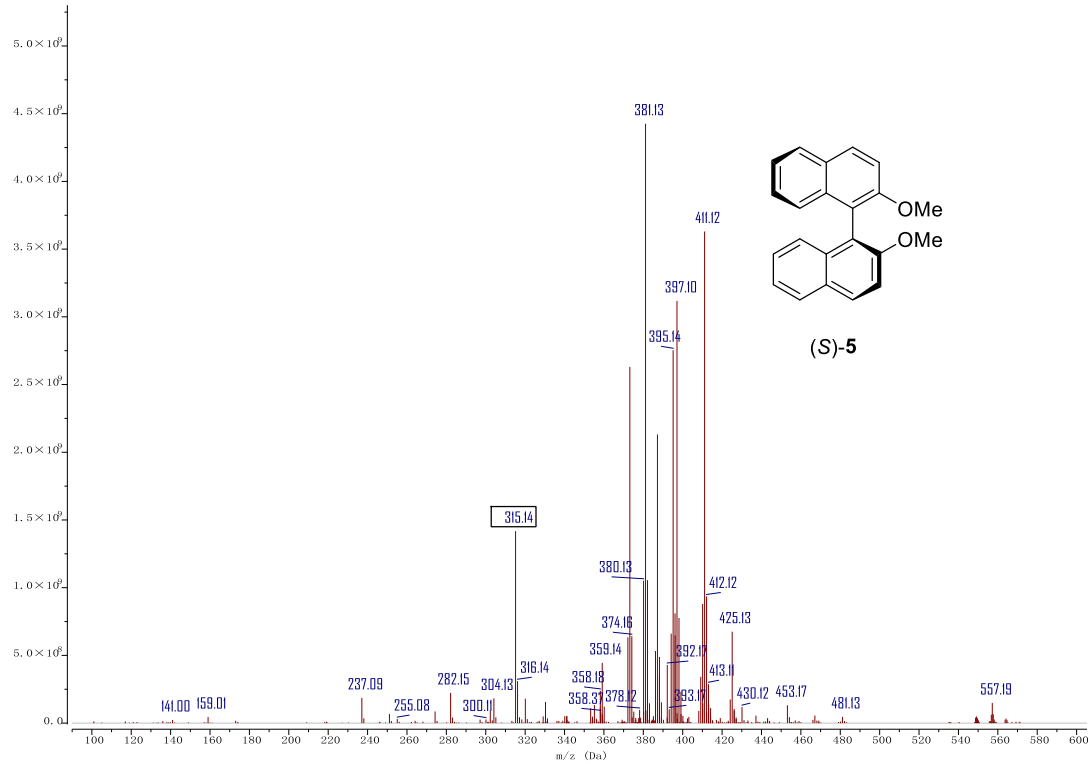

Figure S21. LRMS spectrum of (*S*)-**5**.

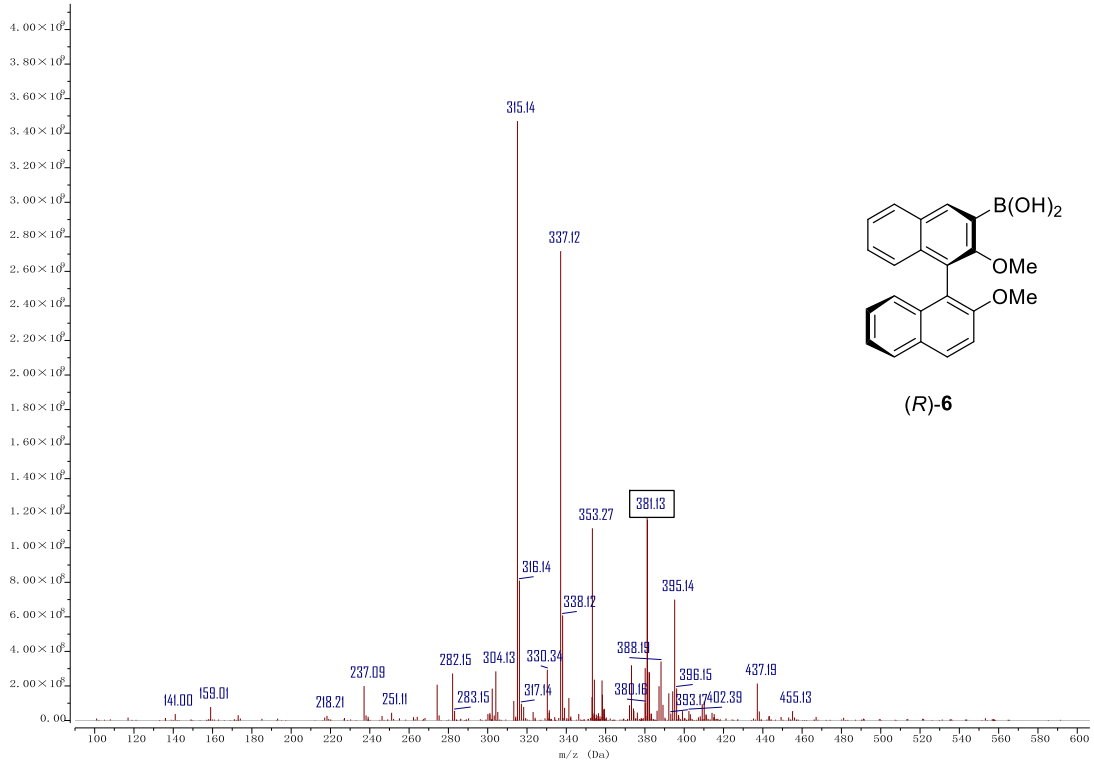

Figure S22. LRMS spectrum of (*R*)-**6**.

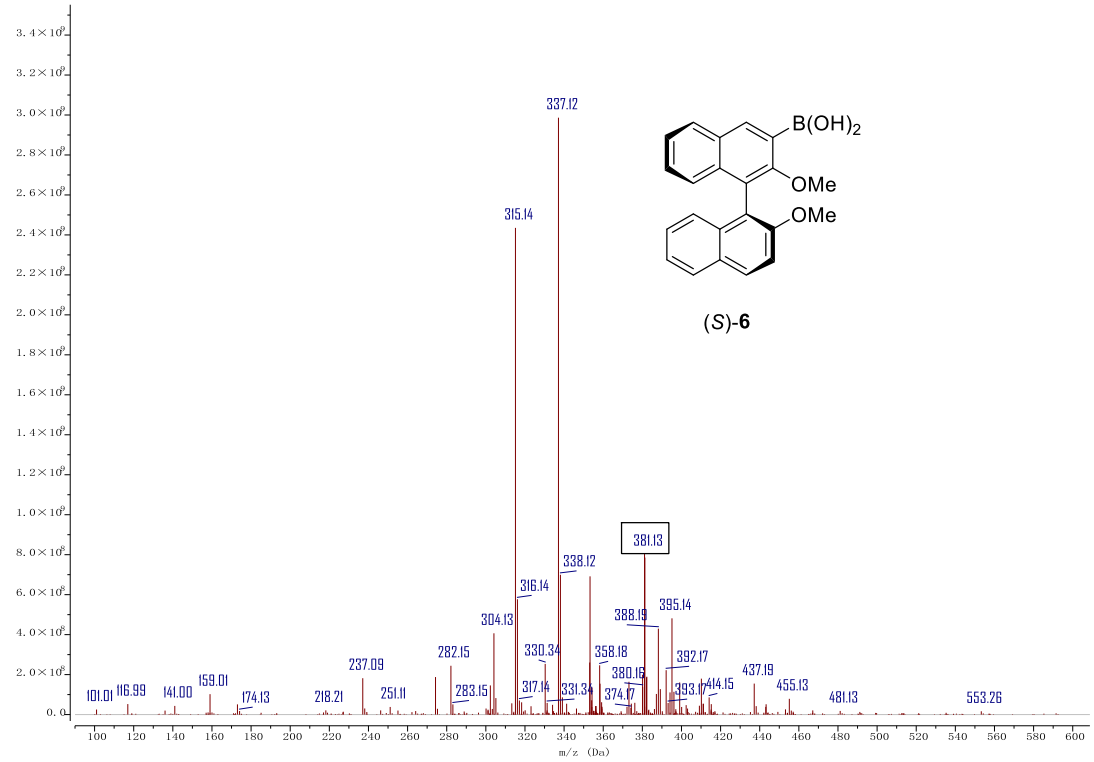

Figure S23. LRMS spectrum of (*S*)-**6**.

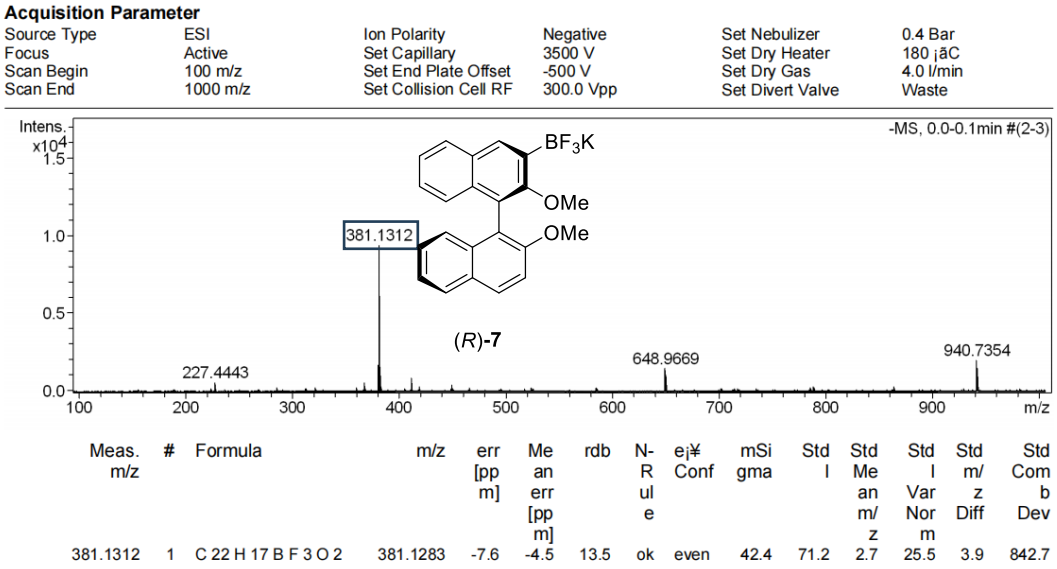

Meas. m/z	#	Formula	m/z	err [ppm]	Mean err [ppm]	rdb	N-Rule	e¡¥Conf	mSigma	Std I	Std Mean m/z	Std I Var Norm	Std m/z Diff	Std Comb Dev
381.1312	1	C 22 H 17 B F 3 O 2	381.1283	-7.6	-4.5	13.5	ok	even	42.4	71.2	2.7	25.5	3.9	842.7

Figure S24. HRMS spectrum of (*R*)-**7**.

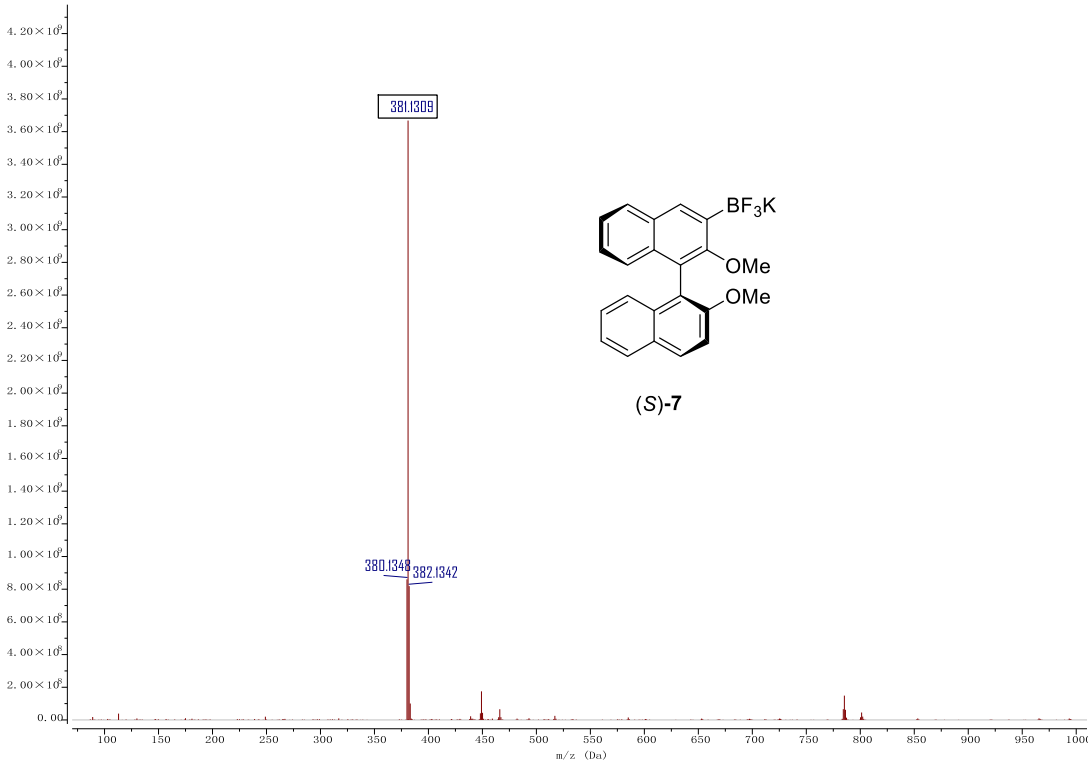

Figure S25 HRMS spectrum of (*S*)-**7**.

Acquisition Parameter

Source Type	ESI	Ion Polarity	Positive	Set Nebulizer	0.4 Bar
Focus	Active	Set Capillary	4500 V	Set Dry Heater	180 ¡ãC
Scan Begin	100 m/z	Set End Plate Offset	-500 V	Set Dry Gas	4.0 l/min
Scan End	1000 m/z	Set Collision Cell RF	300.0 Vpp	Set Divert Valve	Waste

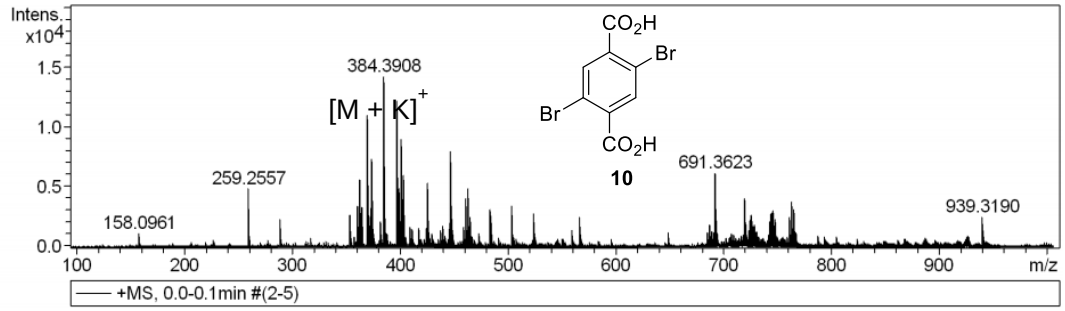

#	m/z	Res.	S/N	I	FWHM
1	259.2557	7953	215.4	4823	0.0326
2	353.2691	6625	48.2	2659	0.0533
3	360.8141	7696	56.8	3404	0.0469
4	362.8113	6710	91.2	5569	0.0541

Figure S26. HRMS spectrum of compound **10**.

Acquisition Parameter

Source Type	ESI	Ion Polarity	Positive	Set Nebulizer	0.4 Bar
Focus	Active	Set Capillary	4500 V	Set Dry Heater	180 ¡ãC
Scan Begin	100 m/z	Set End Plate Offset	-500 V	Set Dry Gas	4.0 l/min
Scan End	1000 m/z	Set Collision Cell RF	300.0 Vpp	Set Divert Valve	Waste

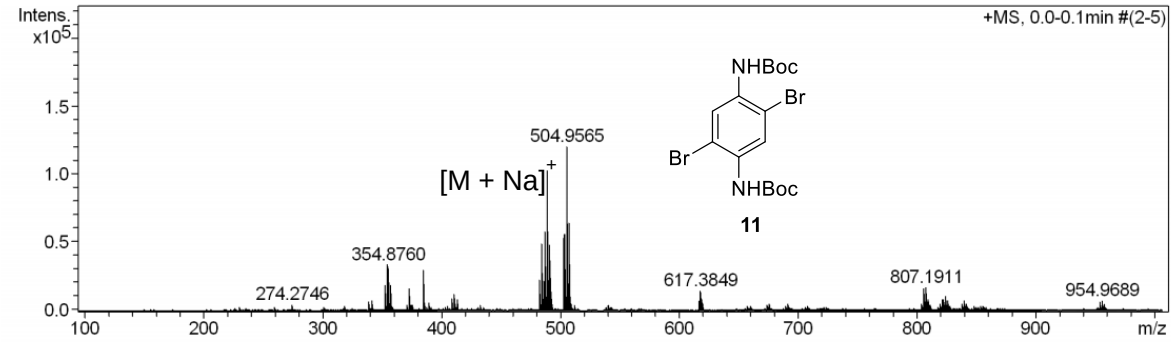

Meas. m/z	#	Formula	m/z	err [ppm]	Mean err [ppm]	rdb	N-Rule	e¡¥Conf	mSigma	Stdl	Std Mean m/z	Std lVarNorm	Std m/z Diff	Std Comb Dev
486.9880	1	C 16 H 22 Br 2 N 2 Na O 4	486.9839	-8.5	-4.5	5.5	ok	even	30.2	33.2	2.7	9.6	2.6	842.7

Figure S27. HRMS spectrum of compound **11**.

Acquisition Parameter

Source Type	ESI	Ion Polarity	Positive	Set Nebulizer	0.4 Bar
Focus	Active	Set Capillary	4500 V	Set Dry Heater	180 ¡ãC
Scan Begin	100 m/z	Set End Plate Offset	-500 V	Set Dry Gas	4.0 l/min
Scan End	1000 m/z	Set Collision Cell RF	300.0 Vpp	Set Divert Valve	Waste

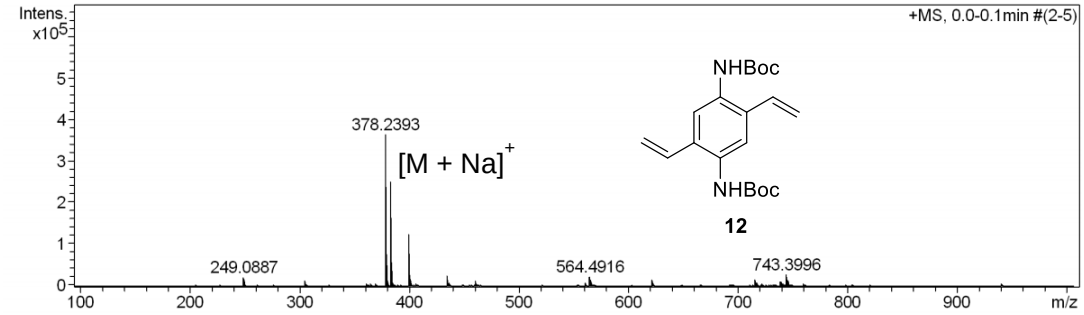

Meas. m/z	#	Formula	m/z	err [ppm]	Mean err [ppm]	rdb	N-Rule	e¡¥Conf	mSigma	StdI	StdMean m/z	StdIVarNorm	Std m/z Diff	Std Comb Dev
383.1953	1	C 20 H 28 N 2 Na O 4	383.1941	-3.0	-2.2	7.5	ok	even	4.4	8.0	1.1	3.5	1.3	842.7

Figure S28. HRMS spectrum of compound **12**.

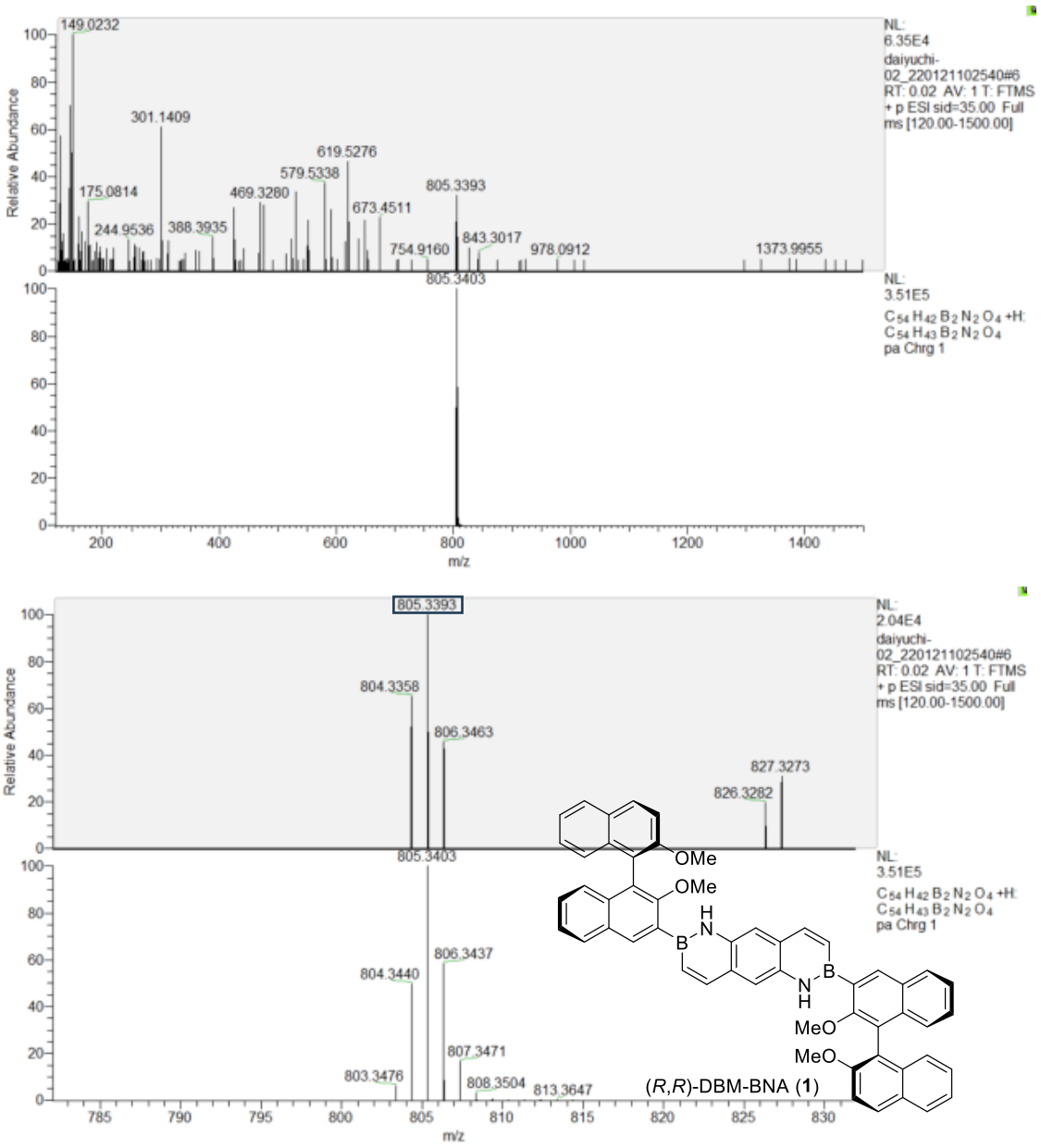

Figure S29. HRMS spectrum of (*R*,*R*)-DBM-BNA (**1**).

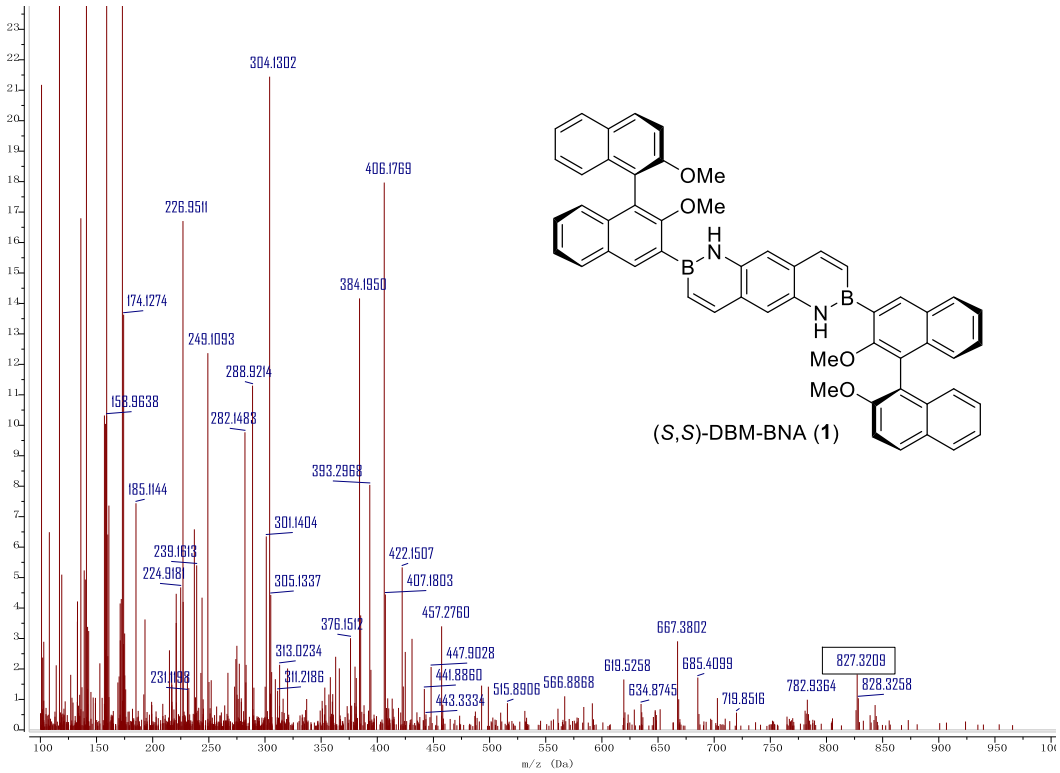

Figure S30. HRMS spectrum of (*S*,*S*)-DBM-BNA (**1**).

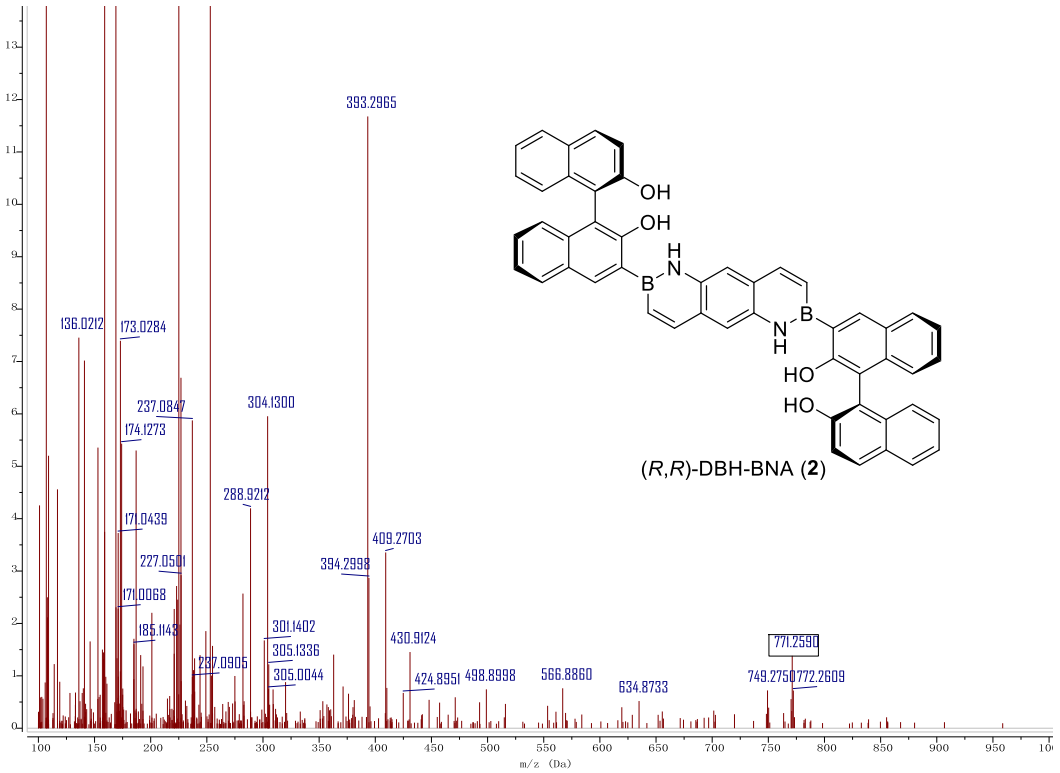

Figure S31. HRMS spectrum of (*R*,*R*)-DBH-BNA (**2**).

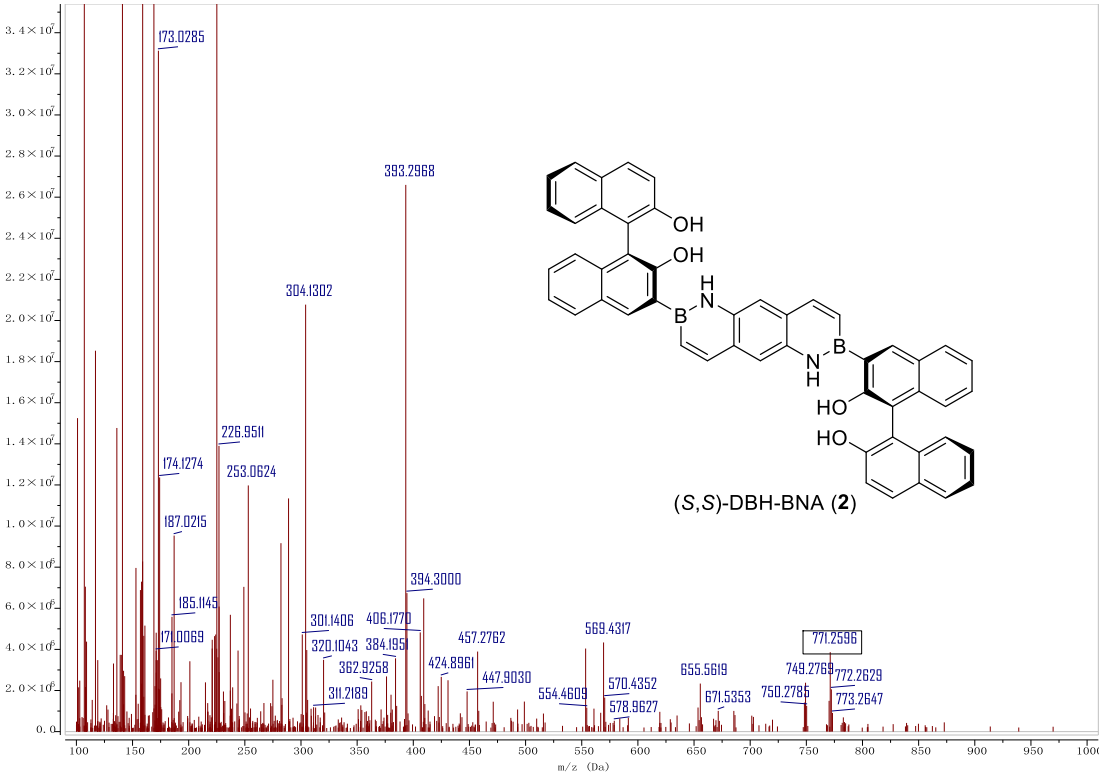

Figure S32. HRMS spectrum of (*S*,*S*)-DBH-BNA (**2**).

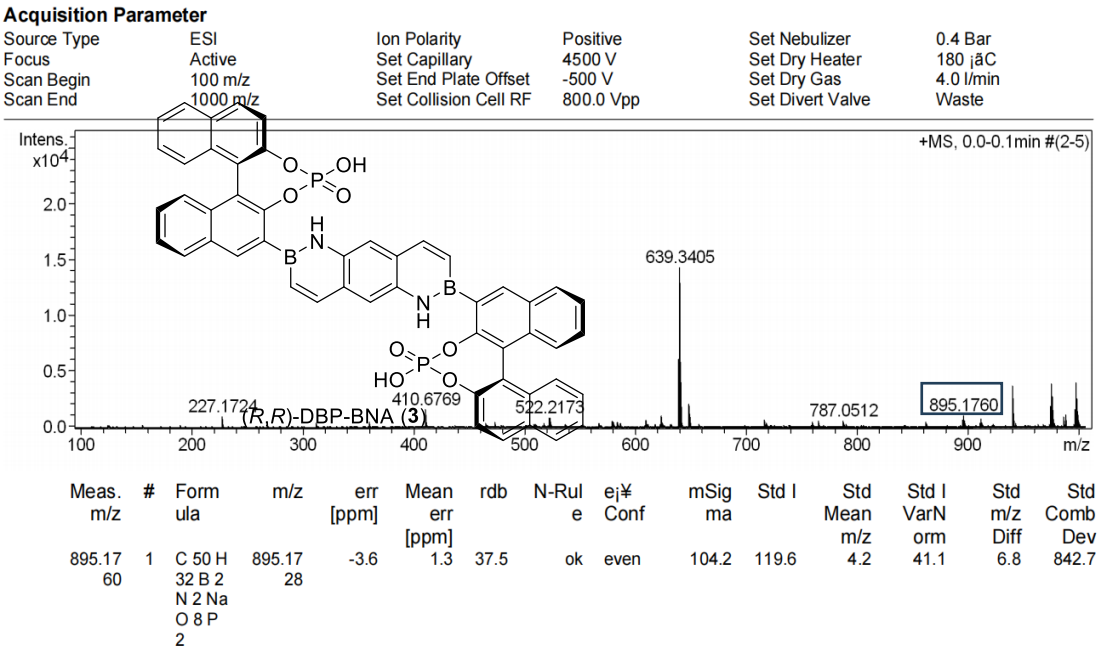

Meas. m/z	#	Formula	m/z	err [ppm]	Mean err [ppm]	rdb	N-Rule	e¡¥Conf	mSigma	Std I	Std Mean m/z	Std I VarNorm	Std m/z Diff	Std Comb Dev
895.1760	1	C 50 H 32 B 2 N 2 Na O 8 P 2	895.1728	-3.6	1.3	37.5	ok	even	104.2	119.6	4.2	41.1	6.8	842.7

Figure S33. HRMS spectrum of (*R*,*R*)-DBP-BNA (**3**).

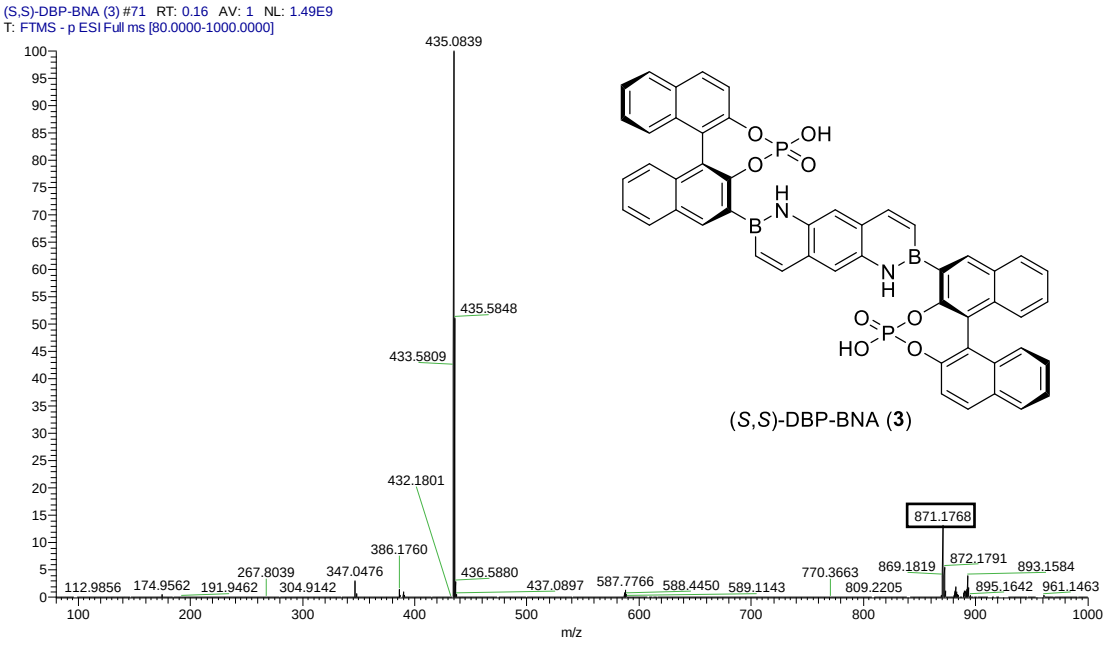

Figure S34. HRMS spectrum of (*S*,*S*)-DBP-BNA (**3**).

5. UV-Vis, FL, circular dichroism and CPL spectra

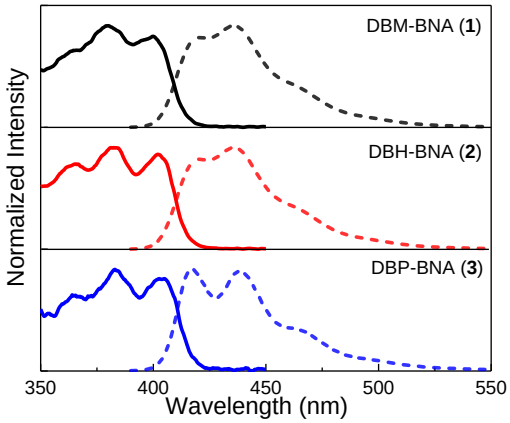

Figure S35. The normalized UV-Vis (solid) and fluorescence (dash) spectra of (*S*,*S*)-DBM-BNA (**1**), (*S*,*S*)-DBM-BNA (**2**) and (*S*,*S*)-DBP-BNA (**3**) in dimethylformamide.

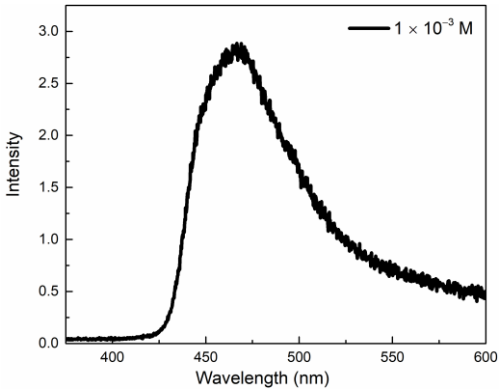

Figure S36. The fluorescence spectra of (*S*,*S*)-DBP-BNA (**3**) in dimethylformamide with the concentration of 1×10^{-3} M.

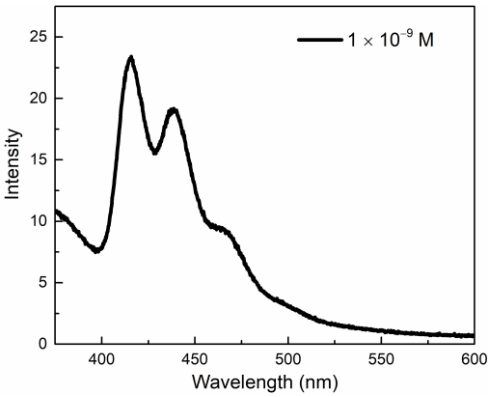

Figure S37. The fluorescence spectra of (*S*,*S*)-DBP-BNA (**3**) in dimethylformamide with the concentration of 1×10^{-9} M.

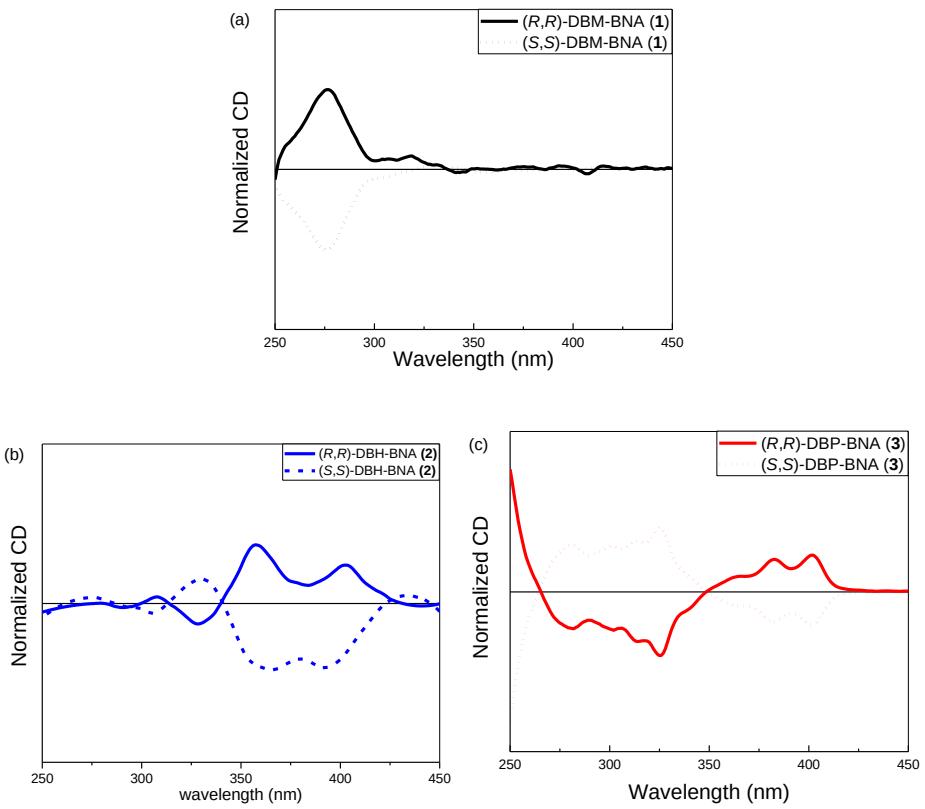

Figure S38. The normalized CD spectra of (a) (*R*,*R*)- or (*S*,*S*)-DBM-BNA (**1**), (b) (*R*,*R*)- or (*S*,*S*)-DBH-BNA (**2**) and (c) (*R*,*R*)- or (*S*,*S*)-DBP-BNA (**3**) in ethyl acetate, $c = 1 \times 10^{-5}$ M, 20 ºC.

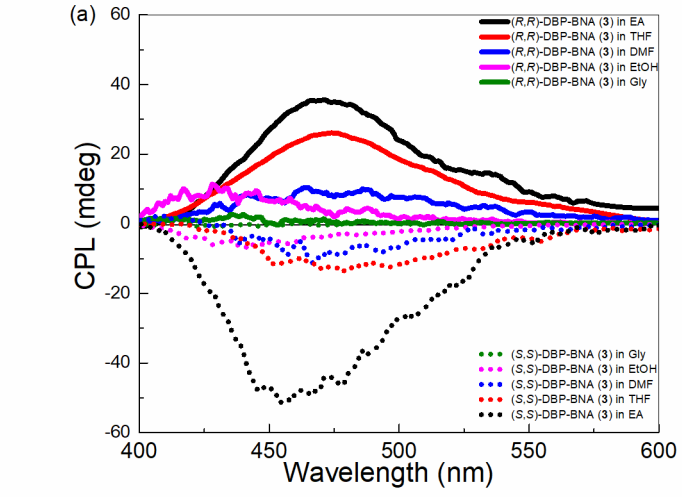

Figure S39. The CPL spectra of (*R*,*R*)- and (*S*,*S*)-DBP-BNA (**3**) in ethyl acetate, tetrahydrofuran, dimethylformamide, ethanol and glycol.

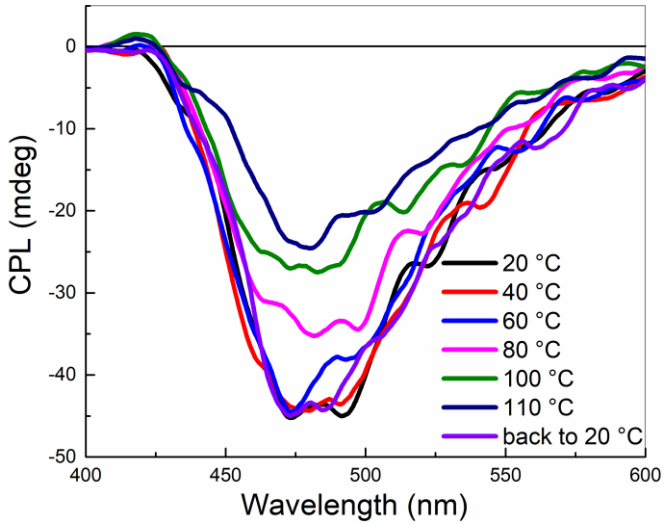

Figure S40. The spectra of CPL signal changed temperature of (*S*,*S*)-DBP-BNA (**3**) from 20 °C to 110 °C and then back to 20 °C. $c = 4 \times 10^{-4}$ M.

Table S1. Experimental Data of DBP-BNA (**3**)

solvent	ε	$\lvert g_{lum} \rvert$	PLQY
DMF	16854	8×10^{-3}	No data
EA	15147	1×10^{-2}	22%
glycol	16050	3×10^{-4}	70%

6. Lifetime data and stimulation

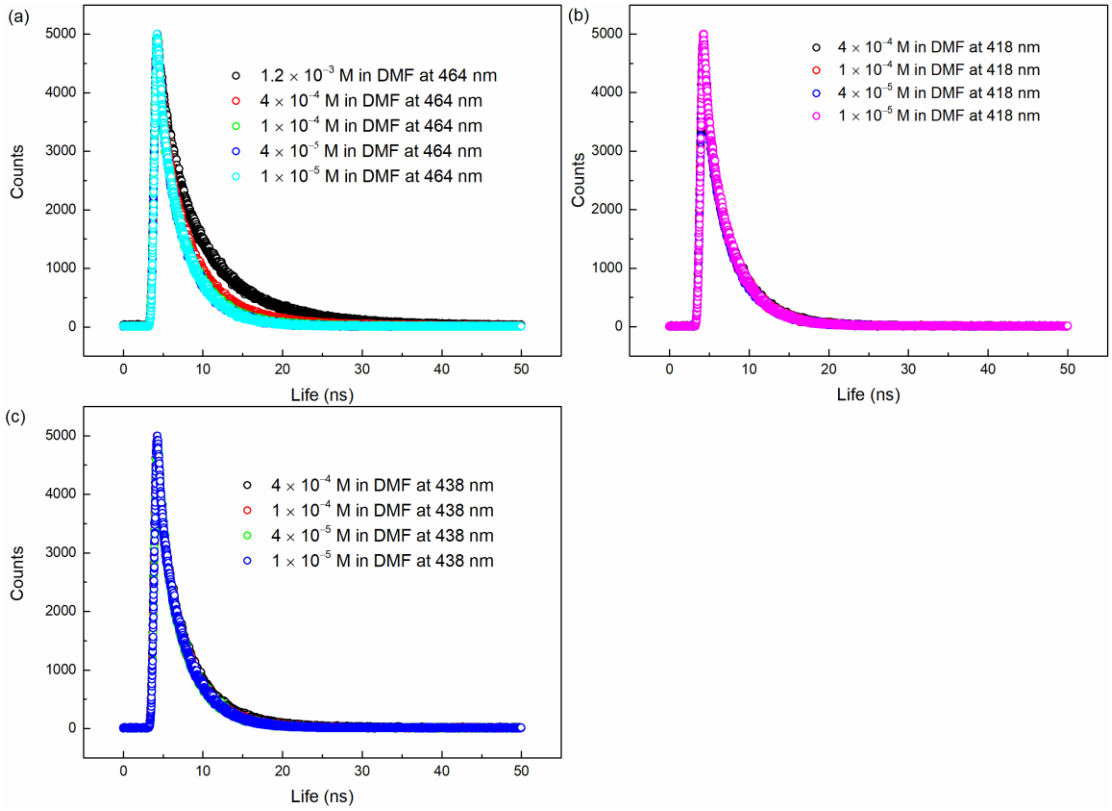

Figure S41. The lifetime of (*S*,*S*)-DBP-BNA (**3**) in *N*,*N*-dimethylformamide with the concentrations of 1.2 × 10^{-3} M, 4 × 10^{-4} M, 1 × 10^{-4} M, 4 × 10^{-5} M and 1 × 10^{-5} M at (a) 464 nm, (b) 418 nm and (c) 438 nm.

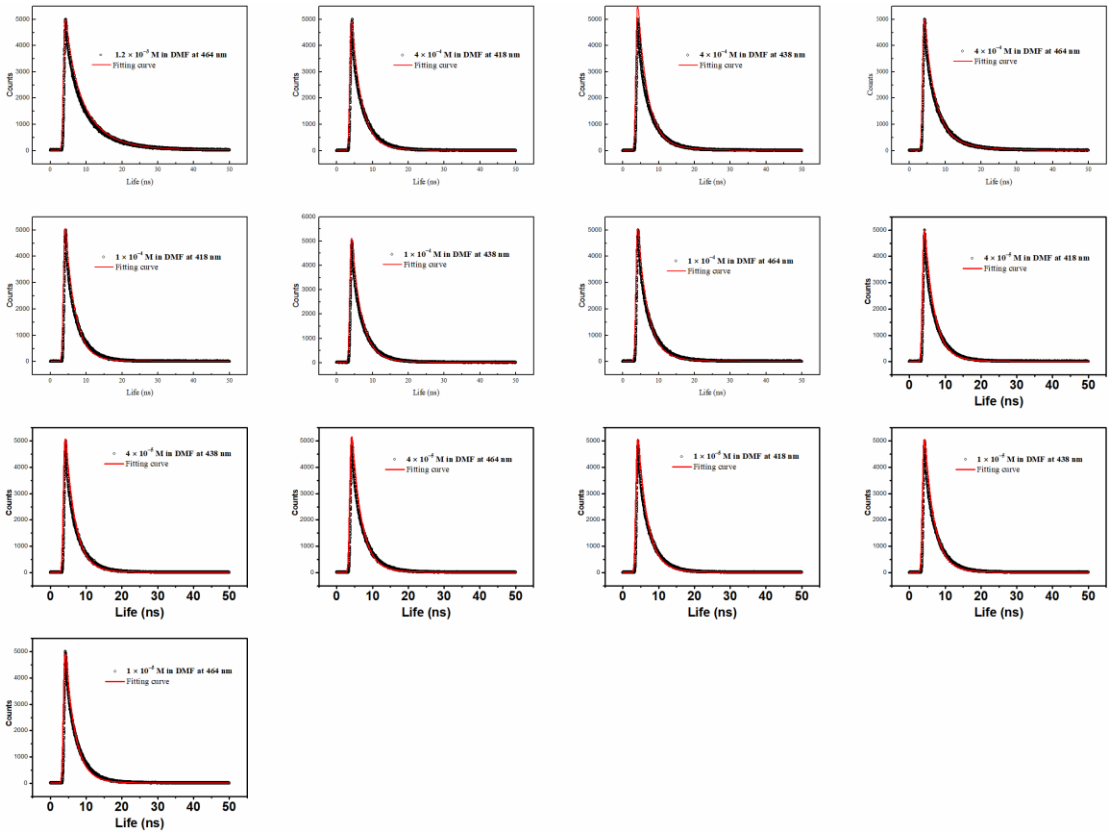

Figure S42. The fitting curve of lifetime of (*S*,*S*)-DBP-BNA (**3**) in DMF at 418 nm, 438 nm and 464 nm.

Table S2. Fitting Parameter of Lifetime in DMF

Entry	Condition	τ_1 (ns)	τ_2 (ns)	C_1	C_2	w_1	w_2	R^2	χ^2
1	1.2×10^{-3} at 464 nm	2.66	7.02	2604	3340	0.438	0.562	0.999	5.434
2	4×10^{-4} at 418 nm	2.66	7.02	6010	292	0.954	0.046	0.999	7.441
3	4×10^{-4} at 438 nm	2.65	7.02	6480	553	0.921	0.079	0.999	5.045
4	4×10^{-4} at 464 nm	2.66	7.02	5166	1121	0.822	0.178	0.999	4.576
5	1×10^{-4} at 418 nm	2.66	7.02	6378	122	0.981	0.019	0.999	3.690
6	1×10^{-4} at 438 nm	2.66	7.02	6301	263	0.960	0.040	0.999	4.913
7	1×10^{-4} at 464 nm	2.66	7.02	6106	361	0.944	0.056	0.999	98.804
8	4×10^{-5} at 418 nm	2.66	7.02	6159	219	0.966	0.034	0.999	6.680
9	4×10^{-5} at 438 nm	2.66	7.02	6311	190	0.971	0.029	0.999	4.878
10	4×10^{-5} at 464 nm	2.66	7.02	6387	233	0.965	0.035	0.999	5.224
11	1×10^{-5} at 418 nm	2.66	7.02	6311	199	0.969	0.030	0.999	5.247
12	1×10^{-5} at 438 nm	2.66	7.02	6310	187	0.971	0.029	0.999	5.337
13	1×10^{-5} at 464 nm	2.66	7.02	6119	186	0.970	0.030	0.999	9.184

7. Theoretical calculations

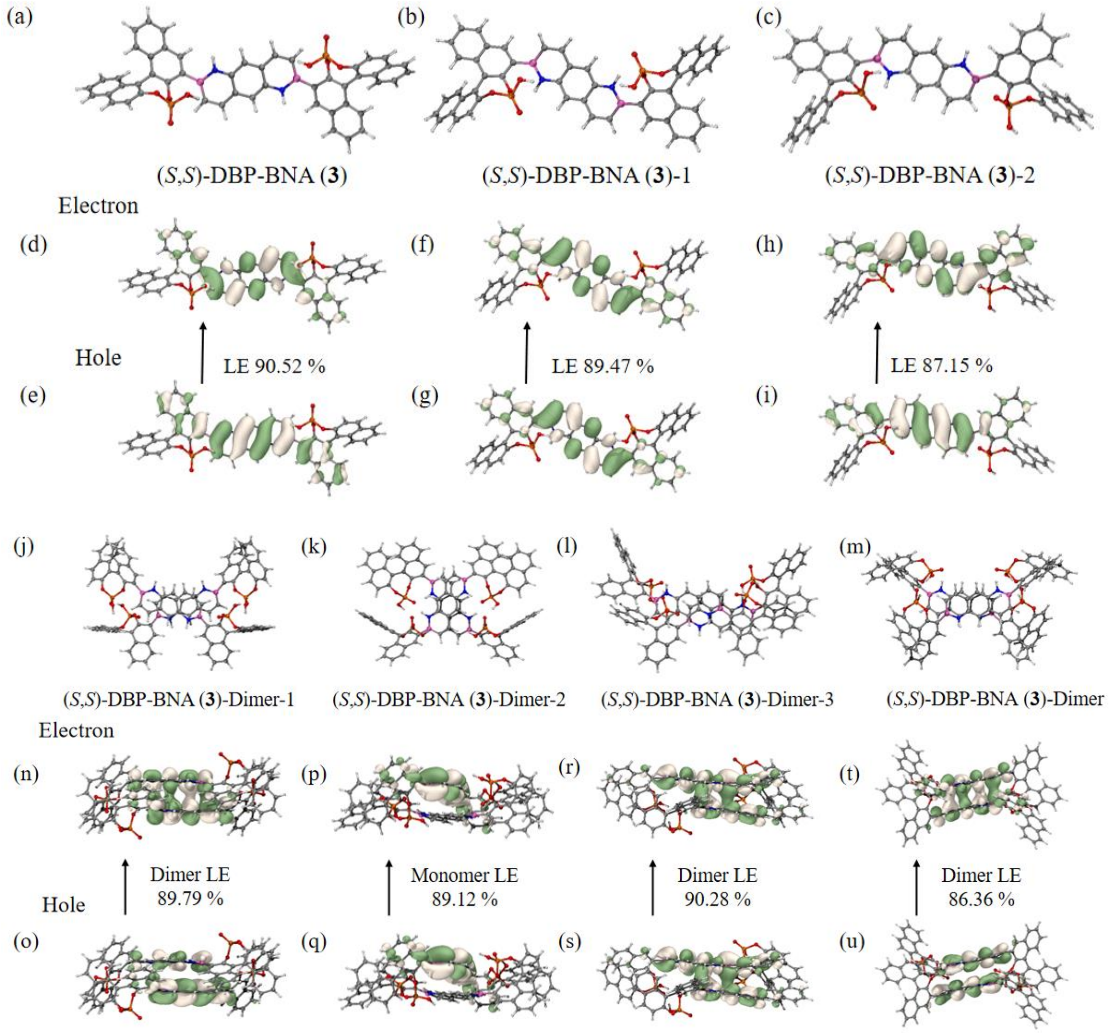

Figure S43. The conformation of the ground states of (a) (*S*,*S*)-DBP-BNA (**3**), (b) (*S*,*S*)-DBP-BNA (**3**)-1, (c) (*S*,*S*)-DBP-BNA (**3**)-2, (d) and (e) are the natural trantransisr orbit of excited state 1 of (*S*,*S*)-DBP-BNA (**3**), (f) and (g) are the natural trantransisr orbit of excited state 1 of (*S*,*S*)-DBP-BNA (**3**)-1, (h) and (i) are the natural transition orbitals of excited state 1 of (*S*,*S*)-DBP-BNA (**3**)-2, (j), (k), (l) and (m) are the possible conformations of dimers, (n), (o), (p), (q), (r), (s), (t) and (u) are the calculation result of the excited state 1 natural transition orbitals of (S,S)-DBP-BNA (**3**) dimer.

Table S3. Theoretical Calculation of S1-DBP-BNA (**3**) Monomers and Dimers

Molecule	S_1 (eV)	f	|μ| (10^{-20} esu·cm)	|M| (10^{-20} erg·G^{-1})	Theta (°)	g (10^{-3})
(*S*,*S*)-DBP-BNA (**3**) [a]	3.24	0.52	652.87	0.41	101.96	-0.52
(*S*,*S*)-DBP-BNA (**3**)-1 [a]	3.35	0.58	675.61	0.38	92.68	-0.11
(*S*,*S*)-DBP-BNA (**3**)-2 [a]	3.36	0.59	683.97	0.62	93.73	-0.23
(*S*,*S*)-DBP-BNA (**3**) in EA [b]	3.03	0.58	711.48	0.38	102.52	-0.46
(*S*,*S*)-DBP-BNA (**3**)-1 in EA [b]	3.19	0.89	859.74	0.41	86.02	0.13
(*S*,*S*)-DBP-BNA (**3**)-2 in EA [b]	3.18	0.80	814.90	0.38	97.07	-0.23
(*S*,*S*)-DBP-BNA (**3**)-Dimer [a]	3.21	0.03	148.23	1.92	180.00	-51.70
(*S*,*S*)-DBP-BNA (**3**)-Dimer-1 [a]	3.17	0.15	355.30	1.92	52.63	13.13
(*S*,*S*)-DBP-BNA (**3**)-Dimer-2 [a]	3.18	0.20	406.85	1.04	69.60	3.58
(*S*,*S*)-DBP-BNA (**3**)-Dimer-3 [a]	2.92	0.04	186.02	2.16	60.63	22.79

a. Optimized ground structure under B3LYP-D3(BJ)/6-31G* level, excited states with TDDFT under CAM-B3LYP-D3(BJ) level.
b. Optimized ground structure under B3LYP-D3(BJ)/6-31G* level with SMD model, solvent = EA, excited states with TDDFT under CAM-B3LYP-D3(BJ) level with SMD model, solvent = EA.

$$g_{lum} = 4\cos\theta\frac{|\mu||m|}{|\mu|^2+|m|^2} \approx 4\cos\theta\frac{|m|}{|\mu|} \quad (\mu \gg m)$$

Table S4 Energy Splitting of Molecules

Dimer	E_{rep} (kcal/mol)	E_{elec} (kcal/mol)	E_{disp} (kcal/mol)	E_{ind} (kcal/mol)	E_{CT} (kcal/mol)
(*S*,*S*)-DBP-BNA (**3**)	34.31	-29.66	-41.73	-4.01	0.00
(*S*,*S*)-DBP-BNA (**3**)-Dimer-1	30.03	-30.05	-51.95	-1.53	0.00
(*S*,*S*)-DBP-BNA (**3**)-Dimer-2	33.43	-30.74	-57.36	-2.18	0.00
(*S*,*S*)-DBP-BNA (**3**)-Dimer-3	46.77	-19.71	-65.33	-2.51	0.00

Table S5 Energy Splitting of Molecules S1(States)

Dimer	E_{rep} (kcal/mol)	E_{elec} (kcal/mol)	E_{disp} (kcal/mol)	E_{ind} (kcal/mol)	E_{CT} (kcal/mol)
(*S*,*S*)-DBP-BNA (**3**)-Dimer-S1	40.35	-28.18	-47.22	-3.53	0.00
(*S*,*S*)-DBP-BNA (**3**)-Dimer-1-S1	33.10	-29.38	-53.12	-1.50	0.02
(*S*,*S*)-DBP-BNA (**3**)-Dimer-2-S1	32.68	-30.73	-55.90	-2.42	0.01
(*S*,*S*)-DBP-BNA (**3**)-Dimer-3-S1	52.01	-18.63	-66.90	-2.55	0.00

Energy Splitting of Dimer $E = E_{rep} + E_{ES} + E_{disp}^{D_4+ATM} + E_{ind} + E_{CT}$

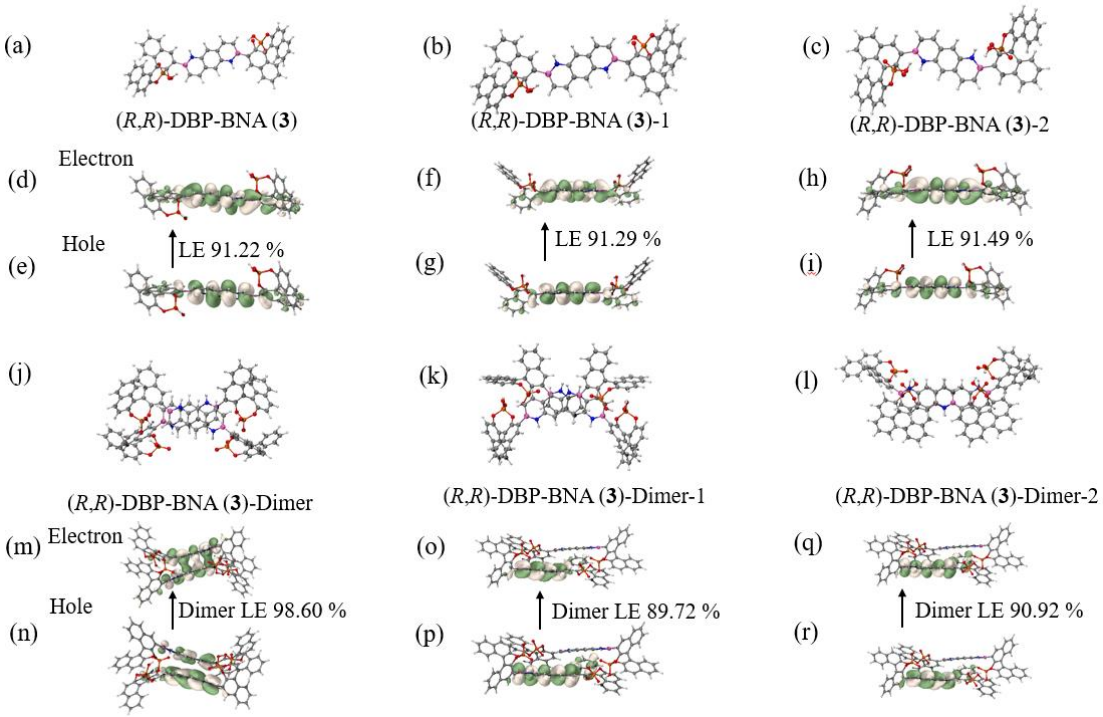

Figure S44. The conformation of the ground states of (a) (*R*,*R*)-DBP-BNA (**3**), (b) (*R*,*R*)-DBP-BNA (**3**)-1, (c) (*R*,*R*)-DBP-BNA (**3**)-2, (d) and (e) are the natural trantransisr orbit of excited state 1 of (*R*,*R*)-DBP-BNA (**3**), (f) and (g) are the natural trantransisr orbit of excited state 1 of (*R*,*R*)-DBP-BNA (**3**), (h) and (i) are the natural transition orbitals of excited state 1 of (*R*,*R*)-DBP-BNA (**3**), (j), (k) and (l) are the possible conformations of dimers, (m), (n), (o), (p), (q) and (r) are the calculation result of the excited state 1 natural transition orbitals of (S,S)-DBP-BNA (**3**) dimer.

Table S6. Theoretical Calculation of S1-DBP-BNA (**3**) Monomers and Dimers

Molecule	S_1 (eV)	*f*	|μ| (10^{-20} esu·cm)	|M| (10^{-20} erg·G^{-1})	Theta (°)	g (10^{-3})
(*R*,*R*)-DBP-BNA (**3**) [a]	3.35	0.59	684.17	0.61	86.22	0.24
(*R*,*R*)-DBP-BNA (**3**)-1 [a]	3.42	0.59	676.54	0.29	103.72	-0.41
(*R*,*R*)-DBP-BNA (**3**)-2 [a]	3.33	0.58	678.02	0.30	87.65	0.07
(*R*,*R*)-DBP-BNA (**3**) in EA [b]	3.20	0.58	800.77	0.35	104.79	-0.45
(*R*,*R*)-DBP-BNA (**3**)-1 in EA [b]	3.17	0.89	761.02	0.15	91.27	-0.02
(*R*,*R*)-DBP-BNA (**3**)-2 in EA [b]	3.20	0.80	854.09	0.29	98.37	-0.20
(*R*,*R*)-DBP-BNA (**3**) -Dimer [a]	3.21	0.03	148.23	1.92	180.00	21.70
(*R*,*R*)-DBP-BNA (**3**) -Dimer-1 [a]	3.16	0.17	373.21	1.93	129.87	-13.27
(*R*,*R*)-DBP-BNA (**3**) -Dimer-2 [a]	3.27	0.34	521.51	1.54	89.98	0.0039

a. Optimized ground structure under B3LYP-D3(BJ)/6-31G* level, excited states with TDDFT under CAM-B3LYP-D3(BJ) level.
b. Optimized ground structure under B3LYP-D3(BJ)/6-31G* level with SMD model, solvent = EA, excited states with TDDFT under CAM-B3LYP-D3(BJ) level with SMD model, solvent = EA.

$$g_{lum} = 4\cos\theta\frac{|\mu||m|}{|\mu|^2+|m|^2} \approx 4\cos\theta\frac{|m|}{|\mu|} \quad (\mu \gg m)$$

Table S7 Energy Splitting of Molecules

Dimer	E_{rep} (kcal/mol)	E_{elec} (kcal/mol)	E_{disp} (kcal/mol)	E_{ind} (kcal/mol)	E_{CT} (kcal/mol)
(*R*,*R*)-DBP-BNA (**3**)-Dimer	34.31	-29.66	-41.73	-4.01	0.00
(*R*,*R*)-DBP-BNA (**3**)-Dimer-1	30.03	-30.05	-51.95	-1.53	0.00
(*R*,*R*)-DBP-BNA (**3**)-Dimer-2	33.43	-30.74	-57.36	-2.18	0.00
(*R*,*R*)-DBP-BNA (**3**)-Dimer-3	46.77	-19.71	-65.33	-2.51	0.00

Table S8 Energy Splitting of Molecules S1(States)

Dimer	E_{rep} (kcal/mol)	E_{elec} (kcal/mol)	E_{disp} (kcal/mol)	E_{ind} (kcal/mol)	E_{CT} (kcal/mol)
(*R*,*R*)-DBP-BNA (**3**)-Dimer-S1	40.35	-28.18	-47.22	-3.53	0.00
(*R*,*R*)-DBP-BNA (**3**)-Dimer-1-S1	33.10	-29.38	-53.12	-1.50	0.02
(*R*,*R*)-DBP-BNA (**3**)-Dimer-2-S1	32.68	-30.73	-55.90	-2.42	0.01
(*R*,*R*)-DBP-BNA (**3**)-Dimer-3-S1	52.01	-18.63	-66.90	-2.55	0.00

Energy Splitting of Dimer $E = E_{rep} + E_{ES} + E_{disp}^{D_4+ATM} + E_{ind} + E_{CT}$

8. References

1. A. Jolit, C. F. Dickinson, K. Kitamura, P. M. Walleser, G.P.A. Yap and M. A. Tius, Catalytic Enantioselective Nazarov Cyclization. *Eur. J. Org. Chem.* 2017, **137**, 6067–6076.
2. T. Gao, Z. Jiang, B. Chen, Q. Sun, Y. Orooji, L. Huang and Z. Liu. Axial Chiral Binaphthalene-Diketopyrrolopyrrole Dyads as Efficient Far-Red to Near-Infrared Circularly Polarized Luminescent Emitters. *Dyes Pigments* 2020, **173**, 107998.
3. J. S. A. Ishibashi, J. L. Marshall, A. Mazière, G. J. Lovinger, B. Li, L. N. Zakharov, A. Dargelos, A. Graciaa, A. Chrostowska and S.-Y. Liu, Two BN Isosteres of Anthracene: Synthesis and Characterization, *J. Am. Chem. Soc.*, 2014, **136**, 15414–15421.